RL-82-112

Science and Engineering Research Council
Rutherford Appleton Laboratory
CHILTON, DIDCOT, OXON, OX11 0QX

RL-82-112

The Theory of Neutron Scattering from Mixed Harmonic Solids

M Warner, S W Lovesey and J Smith

December 1982

THE THEORY OF NEUTRON SCATTERING FROM MIXED HARMONIC SOLIDS

M Warner and S W Lovesey
Rutherford Appleton Laboratory
Chilton, Didcot, Oxon, OX11 0QX

and

J Smith*
Southampton University
Physics Department
Southampton
SO9 5NH

Abstract

The dynamic structure factor for incoherent neutron scattering from light mass particles substituted in a solid is calculated for two model systems. One model is appropriate for a dilute concentration of light particles in a matrix, and the second is a binary system with various masses and force constants. The exact calculations are used to assess the value of approximation schemes for the dynamic structure factor which exploit the separation of time scales in the motions of the light and the heavier lattice particles.

* at Rutherford Appleton Laboratory for the duration of this work.

1. Introduction

There are many materials in which essential chemical and physical properties are revealed in the motion of the constituent hydrogen atoms. Neutron scattering affords a sensitive method for studying hydrogen motion because the scattering cross-section for a bound proton is very large compared with that for many other elements, ie. there is often a very high contrast factor for scattering from hydrogeneous materials. In addition, the single scattering of neutrons is a weak process that can be described within the first Born approximation. In consequence, neutron scattering provides information on the motion of hydrogen atoms which is undistorted by the experimental probe. For these reasons there are many studies of hydrogen motion in solids using thermal neutrons from steady-state reactors [1,2].

Advanced, pulsed neutron facilities have the great advantage of providing intense beams of hot neutrons. Thus, it is feasible to study dynamic processes in which the neutron energy change, ω, is as large as a few electron volts. The concomitant change in the wavevector of the neutron, $\underline{k}$, might also be large compared with values readily obtained in thermal neutron scattering. Since protons in solids usually have a characteristic frequency of oscillation which is large compared with the Debye frequency, we anticipate that the study of hydrogen motion in materials will benefit greatly from the use of hot neutrons from advanced pulsed sources. Questions such as the anharmonicity of the proton potential and intrinsic damping processes might be addressed in greater detail than has been possible hitherto with thermal neutron scattering [3].

A prerequisite to the interpretation of data is a thorough understanding of the behaviour of the scattering from harmonically bound protons. We report some exact theoretical studies of the dynamic structure factor, as a function of $\underline{k}$ and ω, for scattering from light mass particles bound harmonically in a solid. The dynamic structure factor is defined in section 2, together with the standard result for scattering from a particle bound to a fixed (infinite mass) centre. Section 3 contains an analysis of the dynamic structure factor for a single light particle in a matrix of heavier particles. This simple model serves to demonstrate some of the basic features to be expected in the spectrum of a realistic model. An

analysis of a binary system with both various masses and force constants is reported in section 4. Our key results are reviewed in section 5.

2. Basic Theory

Let the position of the light particle at time t be denoted by $\underline{R}(t)$. The spectrum of scattered neutrons is determined by the correlation function [4]

$$F(k,t) = \langle e^{-i\underline{k}\cdot\underline{R}(0)} e^{i\underline{k}\cdot\underline{R}(t)} \rangle \tag{2.1}$$

where the angular brackets denote an ensemble average of the enclosed quantity at a temperature T. For isotropic systems the correlation function depends only upon the magnitude of $\underline{k}$. The dynamic structure factor, or Van Hove function, of central concern is [4],

$$S(k,\omega) = \frac{1}{2\pi}\int_{-\infty}^{\infty} dt\, e^{-i\omega t} F(k,t) \tag{2.2}$$

The structure factor can be calculated exactly for a few systems of interest. These include a free particle in equilibrium, for which [5]

$$F(k,t) = \exp\left\{\frac{k^2}{2m}(it - Tt^2)\right\} \tag{2.3}$$

and

$$S(k,\omega) = \left(\frac{m}{2\pi T k^2}\right)^{1/2} \exp\left\{-\frac{m}{2Tk^2}(\omega - k^2/2m)^2\right\} \tag{2.4}$$

where m is the mass of the particle. We use units in which $\hbar = k_B = 1$. From (2.4) we see that the spectrum is centred about the recoil energy of the particle, $k^2/2m$, and that the Doppler broadening also results in a characteristic width (Γ) of $(k^2T/m)^{\frac{1}{2}}$.

Consider next a particle bound harmonically to a fixed point which defines the centre of coordinates. If the potential is isotropic, and the force constant is $m\omega_o^2$, then [5]

$$F(k,t) = \exp\left\{\frac{k^2}{2m\omega_o} G(\omega_o, t)\right\} \tag{2.5}$$

where

$$G(\omega,t) = i\sin\omega t + (\cos\omega t - 1)\coth(\omega/2T)$$

$$\equiv -\coth(\omega/2T) + \frac{\cosh\{\omega(it + 1/2T)\}}{\sinh(\omega/2T)} \tag{2.6}$$

The Fourier transform of F(k,t) is readily obtained using the second form for G(ω,t) in (2.6) and the generating function for modified Bessel functions of the first kind, I_n. The result is,

$$S(k,\omega) = \exp\{-2W\} \sum_{-\infty}^{+\infty} I_n(y) \exp\left(\frac{n\omega_o}{2T}\right) \delta(\omega - n\omega_o) \tag{2.7}$$

where exp(-2W) is the Debye-Waller factor, and the delta function expresses conservation of energy on exciting (n > 0) or annihilating (n < 0) many quanta. The argument of the Bessel function is,

$$y = k^2 / \{2m\omega_o \sinh(\omega_o/2T)\} \tag{2.8}$$

and

$$2W = (k^2/2m\omega_o)\coth(\omega_o/2T) \tag{2.9}$$

We note that if $y \ll 1$, achieved either for $k^2 \ll m\omega_o$ or for $T \ll \omega_o$, then for $n \geq o$,

$$I_n(y) \longrightarrow (y/2)^n/n! \tag{2.10}$$

with $I_n = I_{-n}$ for integer n. Thus, in the limit $y \to 0$ only the elastic ($n = 0$) term is significant. The limit $T \ll \omega_o$ is discussed more specifically at equation (2.23).

In the opposite limit, $y \gg 1$, which arises for $k^2 \gg m\omega_o$ or $T \gg \omega_o$, $I_n(y)$ becomes independent of n, namely,

$$I_n(y) \longrightarrow (2\pi y)^{-1/2}\exp(y) \tag{2.11}$$

Hence, for $k^2 \gg m\omega_o$,

$$\exp(-2W)I_n(y) \longrightarrow (2\pi y)^{-1/2}\exp\left\{\frac{-k^2}{2m\omega_o}\tanh(\omega_o/2T)\right\} \tag{2.12}$$

whereas in the limit of high temperatures, $T \gg \omega_o$,

$$\exp(-2W)I_n(y) \longrightarrow (2\pi y)^{-1/2} \tag{2.13}$$

with

$$y \longrightarrow \left(k^2/2m\omega_o\right)\left(2T/\omega_o\right) \tag{2.14}$$

We conclude that for $y \gg 1$ all inelastic events contribute to the dynamic structure factor but the amplitude of each contribution is small, particularly if the wavevector is large so that $k^2 \gg m\omega_o$.

The above analysis shows with what weight the n^{th} oscillator line enters into the dynamic structure factor in the limit of large y, ie. recoil energy, $k^2/2m$, large compared with ω_o or high temperatures T. Ultimately as the ratio ω/ω_o becomes large, or alternatively as the interaction time becomes short, the neutron will perceive the light particle as free. This limit is the impulse approximation and is important in the examination of various approximation schemes to be analysed below. The overall shape of the dynamic structure factor in the short-time limit can be easily calculated by expanding the function $G(\omega_o,t)$, in the exponent of the expression for $F(k,t)$, for small times $t \ll 1/\omega_o$

$$G(\omega_o,t) = i\omega_o t - \coth\left(\omega_o/2T\right)\frac{\omega_o^2 t^2}{2} + O(t^3) \quad (2.15)$$

whence F(k,t) becomes

$$F(k,t) = \exp\left(itk^2/2m - \tfrac{1}{2}t^2\Gamma^2 + O(t^3)\right) \quad (2.16)$$

with

$$\Gamma^2 = \left(k^2\omega_o/2m\right)\coth\left(\omega_o/2T\right) \quad (2.17)$$

The dynamical structure factor is obtained by Fourier transformation of F(k,t). For the expansion (2.15) to be useful one must not only fulfill the condition $t \lesssim 1/\omega_o$ for its validity but also have the decay of the Gaussian term before times of order $t \sim 1/\omega_o$, that is, the condition below must hold:

$$\tfrac{1}{2}\left(k^2\omega_o/2m\right)\coth\left(\omega_o/2T\right)/\omega_o^2 \gg 1$$

or $$k^2/2m \gg 2\omega_0 \coth(\omega_0/2T) \tag{2.18}$$

which is easily satisfied under conditions of high energy transfer. With these restrictions $S(k,\omega)$ becomes

$$S(k,\omega) = (1/2\pi\Gamma^2)^{1/2} \exp\{-(\omega - k^2/2m)^2/2\Gamma^2\} \tag{2.19}$$

Thus the dynamic structure factor is a Gaussian displaced by the free particle recoil and with a characteristic width Γ. It is interesting to cast Γ in terms of the free particle width function of (2.4):

$$\Gamma = \Gamma_{fp} \cdot \sqrt{(\omega_0/2T)\coth(\omega_0/2T)} \tag{2.20}$$

where the second equality defines Γ_{fp}, the characteristic width in (2.4).

For $\omega_0 \to 0$, that is the softening of the harmonic potential, the free particle width is obtained. For $\omega_0/2T > 0$ the factor $\sqrt{\frac{\omega_0}{2T} \cdot \coth\frac{\omega_0}{2T}}$ rapidly produces an increase of Γ over and above the free particle result eg. for $\omega_0/2T \sim 5$ we have $\Gamma \sim 2\Gamma_{fp}$. This is often interpreted as the particle having an effective temperature.

$$T \cdot (\omega_0/2T)\coth(\omega_0/2T) > T \tag{2.21}$$

or as having an effective mass

$$m/\{(\omega_0/2T)\coth(\omega_0/2T)\} \leq m \tag{2.22}$$

The case of low temperatures, $T \ll \omega_0$ merits special attention. For $T \to 0$, and $n \geq 0$,

$$\exp(-2W) I_n(y) \exp(n\omega_0/2T) \longrightarrow \exp(-z) \cdot z^n/n! \qquad (2.23)$$

where the dimensionless variable

$$z = k^2/2m\omega_0 \ .$$

The optimum amplitude of the n^{th} process is obtained for $z = n$, and the amplitude decreases slowly with increasing n. Thus, the higher harmonics will make a significant contribution to the structure factor when the temperature is decreased to make $y \ll 1$. The optimal scattering vector for the n^{th} process is $k^2 = 2nm\omega_0$.

3. Single Light Scatterer

A realistic model must allow the lattice particles to participate in the motion and this is achieved for a finite value of the ratio of the light mass to the heavier mass of the lattice particles. The reaction of the lattice to the motion of the light particle of interest will modify the dynamic structure factor, just as a heat bath influences the motion of an immersed particle and produces a Doppler broadening of the spectrum. Here we consider the simplest example of this coupled motion, namely a lattice of harmonically bound particles of mass M and one substitute of mass $m < M$. This model will be adequate for the description of scattering from a dilute concentration of light particles.

The motion of the light particle can be calculated in terms of the vibrational density of states of the (pure) system in which all particles have the same mass, M [5]. The mixed system supports a high frequency mode of vibration for a sufficiently small mass ratio; this is often referred to as a localised impurity mode. If we denote the pure host density of states by $Z(\omega)$, then the frequency of the localised mode, ω_0, is determined by the equation

$$1/\lambda = \omega_0^2 \int_0^{\theta} d\omega \; Z(\omega) / (\omega_0^2 - \omega^2) \tag{3.1}$$

where the perturbation parameter

$$\lambda = 1 - m/M \tag{3.2}$$

In (3.1) $\omega_0 > \theta$ where θ is the cut-off in the density of states. When we have $\omega_0 < \theta$, as for instance in (3.7) below, we take the principal part of the integral in (3.1). The maximum value of m/M at which a solution of (3.1) exists depends on the precise form of $Z(\omega)$.

An analytic calculation is possible for the Debye density of states,

$$\begin{aligned} Z(\omega) &= 3\omega^2/\theta^3 \qquad |\omega| < \theta \\ &= 0 \qquad\qquad |\omega| > \theta \end{aligned} \tag{3.3}$$

For this vibrational density of states a localised mode exists for $m < M$. Equation (3.1) for ω_0 reduces to

$$1/\lambda = 3x_0^2 \left\{ \frac{x_0}{2} \ln \left| \frac{x_0 + 1}{x_0 - 1} \right| - 1 \right\} = f(x_0) \tag{3.4}$$

where $x_0 = \omega_0/\theta$. The value of x_0 increases as the mass ratio decreases, and for $(m/M) \ll 1$ the solution is

$$\omega_0^2 \doteq (3\theta^2/5)(M/m) \tag{3.5}$$

Let us turn now to the calculation of the dynamic structure factor for the light particle. In the definition of the correlation function F(k,t), equation (2.1), $\underline{R}$ is then the displacement of the particle from its equilibrium position, and

$$F(k,t) = \exp\left\{ \frac{k^2 h(x_0)}{2m\omega_0} G(\omega_0,t) + \right.$$
$$\left. + k^2/2M \int_0^\Theta du\, Z(u) G(u,t)/u D(u) \right\} \qquad (3.6a)$$

where

$$D(u) = \left\{ 1 - \lambda f(u/\Theta) \right\}^2 + \left\{ \frac{1}{2} \lambda \pi u Z(u) \right\}^2 \qquad (3.6b)$$

and where G is defined in equation (2.6).

Notice that the correlation function is the product of two factors. The first factor arises from the high frequency vibration of the light particle, and the second factor is the contribution of the lattice vibrations. The function h(x) in the first factor is the amplitude of the high frequency mode, and it vanishes for $\omega_0 \to \Theta$ which occurs for $m \to M$. For the Debye density of states, and $x = \omega/\Theta$,

$$h(x) = f(x)\left\{ f(x) - 1 \right\}/g(x) \qquad (3.7)$$

where f(x) is defined in equation (3.4) and

$$g(x) = \frac{3x^2}{2}\left\{ 3 + \frac{1}{(x^2-1)} - \frac{3x}{2} \ln\left| \frac{x+1}{x-1} \right| \right\} \qquad (3.8)$$

The function (3.7) is plotted in figure (1), from which it is seen that $h(x_o)$ rapidly achieves its saturation value as ω_o moves away from θ, ie. as m/M decreases. From the behaviour of h(x) it follows that, as we should expect, the result (3.6) coincides with (2.5) in the limit $(m/M) \to 0$.

The significance of the lattice contribution to (3.6) is perhaps best appreciated by considering an approximation to F(k,t) which might, at first sight, be expected to be excellent for $\omega_o \gg \theta$. In this limit, which is achieved for $m \ll M$, the distinct separation in time scales for the motions of the light and lattice particles should mean that there is minimal dynamical coupling between the two forms of motion. Under such conditions, the correlation function would be a product of the correlation function for the motion of the light particle,

$$\exp\left\{\frac{k^2}{2m\omega_o} G(\omega_o,t)\right\} \tag{3.9}$$

and the vibrations of the lattice particles, namely

$$\exp\left\{\frac{k^2}{2M}\int_0^\theta du\, Z(u)\, G(u,t)/u\right\} \tag{3.10}$$

The first step in this approximation scheme is indeed excellent, because $h(\omega_o)$ approaches unity rapidly with increasing ω_o. However, (3.10) is not a good approximation for the lattice contribution because the exact result (3.6) shows that the density of states in the integrand is reduced significantly for $\lambda \lesssim 1$ by the factor $D^{-1}(u)$. We shall consider this point in more detail after discussing the dynamic structure factor.

It is not possible to calculate the time Fourier transform of F(k,t) in analytic form. However, we can readily obtained the form of $S(k,\omega)$ for $\omega \to 0$ and $\omega \gg \theta$. For small ω, we need to consider the long-time behaviour of F(k,t). The time dependence is contained in $G(\omega,t)$, equation (2.6), which consists of a constant term, and sinusoidal terms that oscillate rapidly about zero for large values of t. Hence, in this limit we can expand the exponentials in terms of the sinusoidal functions to obtain, for $\omega \to 0$,

$$S(k,\omega) \doteq \exp\{-2W_0 - 2W_L\} \cdot \{\delta(\omega) + (k^2/2M)\, T\, Z(\omega)/\omega^2\Big|_{\omega=0} + \cdots\} \tag{3.11}$$

Here, $2W_0$ is obtained from (2.9) on multiplying by $h(x_0)$, and

$$2W_L = (k^2/2M)\int_0^\theta du\, Z(u) \coth(u/2T)/u\, D(u) \tag{3.12}$$

Thus, the structure factor for $\omega \to 0$ consists of an elastic line on a background depending linearly on temperature. The amplitude is given by the product of Debye-Waller factors for the light mass and lattice contributions.

As an example, we consider the magnitude of the various terms for (m/M) = 0.10 and a Debye density of states. For this mass ratio, $\omega_0 = 2.5\theta$, $h(x_0) = 0.98$ and for $T \gtrsim \theta$

$$2W_L \doteq (k^2/2M)(6T/\Theta^2) * 0.46 \tag{3.13}$$

Hence the exponent in the Debye-Waller factor for the lattice contributions is reduced to less than one half of the naive estimate based on a simple Debye density of states and ignoring the λ dependent terms, ie. D(u).

Next we consider $S(k,\omega)$ for $\omega \gg \theta$. The behaviour of $S(k,\omega)$ in this limit is determined by the short-time values of $F(k,t)$. Since the limit $\omega \gg \theta$ may be achieved with $\omega \sim \omega_0$ we expand $G(u,t)$ in t and keep the full form for $G(\omega_0,t)$. Retaining terms up to t^2 in $G(u,t)$, ie. the leading order terms of its real and imaginary components, and again using the generating function for the Bessel functions I_n to rewrite $\exp\{G(\omega_0,t)\}$, we arrive at the result, valid for $\omega \gg \theta$,

$$S(k,\omega) \doteq (2\pi\Gamma^2)^{-1/2} \exp(-2W_0) \cdot \sum_{n=-\infty}^{+\infty} I_n(y) \exp\left(n\omega_0/2T - (q+n\omega_0-\omega)^2/2\Gamma^2\right) \tag{3.14}$$

The functions Γ^2 and q are defined by,

$$\left.\begin{matrix}\Gamma^2 \\ q\end{matrix}\right\} = \frac{k^2}{2M}\int_0^{\theta} \frac{du\, Z(u)}{D(u)} \left\{\begin{matrix} u\coth(u/2T) \\ 1\end{matrix}\right. \tag{3.15}$$

and y and $2W_0$ are obtained from (2.8) and (2.9) by multiplying by $h(x_0)$. The lattice contribution is seen to produce a shift and width in the harmonic oscillator line resulting from the motion of the light mass particle considered alone. Both Γ^2 and q are proportional to $k^2/2M$, and q is temperature independent.

The integral in the definition of q can be expressed in terms of the amplitude of the high frequency mode, $h(x_0)$. From the sum rule [17],

$$\int_{-\infty}^{+\infty} d\omega\, \omega\, S(k,\omega) = k^2/2m \tag{3.16}$$

we find an expression which in effect represents the conservation of the total number of states,

$$\int_0^{\theta} \frac{du\, Z(u)}{D(u)} = \frac{M}{m}\left\{1 - h(x_0)\right\} \tag{3.17}$$

This expression follows directly from the structure of the result (3.6) for the correlation function, and it does not rely on the specific density of states. For the Debye density of states we find that, using (3.7) for $h(x_0)$, the right-hand side of (3.17) achieves a minimum value of 4/21 in the limit $(m/M) \to 0$. Hence,

$$0.190 \leq \int_0^{\theta} \frac{du\, Z(u)}{D(u)} \leq 1.0 \tag{3.18}$$

where the upper limit is achieved for m=M at which D(u) = 1. Thus, in the limit (m/M) → 0, the shift in the positions of the peaks in (3.14) tends to the result

$$q \rightarrow (k^2/2M) * 0.19 \tag{3.19}$$

For temperatures $T \gtrsim \theta$, then $\Gamma^2 \simeq 2Tq$ to a good approximation. We therefore conclude that the shift and damping of the harmonic oscillator lines is minimal for $\omega_0 \gg \theta$, which is achieved for $m \ll M$.

Notice that we obtain quite different results if we consider the limit $k^2 \rightarrow \infty$. In this instance we should argue that, since k^2 is a factor in the lattice and light particle contributions in the correlation function, both contributions in the correlation function (3.6) are expanded to order t^2 and not just the lattice contribution as in (3.14). The result for $k^2 \rightarrow \infty$ is then,

$$F(k,t) \doteq \exp\left\{ i t k^2/2m - k^2 t^2 \langle v^2 \rangle / 6 \right\} \tag{3.20}$$

where $\underline{v}$ is the velocity of the particle, and we have used (3.17). From (3.20) it follows at once that the dynamic structure factor is centred about the recoil energy of the light particle, and the width of the spectrum is proportional to $(k^2 \langle \underline{v}^2 \rangle)^{\frac{1}{2}}$. If the temperature is such that $\Gamma^2 = 2Tq$ to a good approximation, we find

$$\langle \underline{v}^2 \rangle = \left(\frac{3T}{m}\right)\left\{ 1 - h(x_0) + \frac{h(x_0)}{2T} \omega_0 \coth(\omega_0/2T) \right\} \tag{3.21}$$

in which the term $1-h(x_0)$ is negligible for $(m/M) \ll 1$.

The result (3.20) is equivalent to the impulse approximation. To show this it is convenient to use an alternative form for the correlation function [6]

$$F(k,t) = \exp\left\{\frac{itk^2}{2m}\right\} \left\langle \hat{T} \exp\left\{ik \cdot \int_0^t dt' \, v(t')\right\}\right\rangle \quad (3.22)$$

in which $\hat{T}$ is the time-ordering operator. The impulse approximation is obtained from (3.22) in the limit $k^2 \to \infty$. Noting that in this limit $F(k,t)$ is negligible except when t is small, we can expand the integral in (3.22) to get:

$$F(k,t) \doteq \exp\left\{\frac{itk^2}{2m}\right\} \left\langle \exp\left(itk \cdot v(0)\right)\right\rangle$$

$$= \exp\left(-itk^2/2m - t^2 \langle (k \cdot v(0))^2 \rangle / 2\right) \quad (3.23)$$

where the equality is strictly valid for systems in which the interactions are harmonic [7]. Corrections to the impulse approximation are obtained by taking further terms in the Taylor series expansion of the argument of the second exponential in (3.22), that is:

$$t\,v(0) + t^2 \dot{v}(0)/2! + t^3 \ddot{v}(0)/3! + \cdots$$

The first correction contains contributions from terms up to the order t^3, and the corresponding result, on the Fourier transforming $F(k,t)$, for the dynamic structure factor is $(k^2 \to \infty)$

$$S(k,\omega) \doteq \left\{2\pi / \langle (k \cdot v)^2 \rangle\right\}^{1/2} \exp\left(-\varepsilon^2\right) \cdot$$

$$\cdot \left\{1 + \left[\langle \dot{v}^2 \rangle / (8k^2 \langle v^2 \rangle)\right](4\varepsilon^4 - 12\varepsilon^2 + 3)\right\} \quad (3.24)$$

where the dimensionless variable

$$\varepsilon = (\omega - k^2/2m) / (2\langle (\underline{k}\cdot\underline{v})^2 \rangle) \tag{3.25}$$

and $\underline{\dot{v}} \equiv \underline{\dot{v}}(0)$ is the acceleration of the particle. Hence the coefficient of the first correction to the impulse approximation is proportional to the average of the square of the force on the light mass particle. The correction to the impulse approximation tends to make the dynamic structure factor more Lorentzian in shape as a function of ε. For $m \ll M$ we find that

$$\langle \underline{\dot{v}}^2 \rangle / (8k^2 \langle \underline{v}^2 \rangle^2) \doteq m\omega_0 / (12k^2 \coth(\omega_0/2T)) \tag{3.26}$$

and this must be small for the approximation (3.24) to be valid.

In closing this section we note that $\langle \underline{v}^2 \rangle$ can be calculated from the free energy for a system as a function of mass and force constant using a relation derived by Maradudin, Flinn and Ruby [8].

4. Binary System; preliminaries

We turn now to the study of a binary system with masses and force constants that we vary to explore a range of different regimes. This is a simple model of a situation frequently encountered in chemical spectroscopy, where the light scatterer is bound in a molecule which is itself bound in a lattice. The vibrational density of states consists of two distinctly different components (when the masses and force constants are sufficiently dissimilar). At low frequencies there is a broad spectrum that is proportional to ω^2 for $\omega \to 0$ and terminates at θ, which arises primarily from the vibrations of the heavy lattice particles. The second component arises from the vibrations of the light particles; it is centred at a frequency that is large compared with θ, and it has a width which is small

compared with θ. We shall often refer to these two components of the vibrational density of states as the lattice and oscillator, or low and high frequency, bands. For the case of a single light substitute, considered in the previous section, the oscillator band is infinitely narrow and corresponds to an Einstein oscillator. Looking ahead to the density of states calculated for our binary system, an example of which is shown in figure (2), we may see that the oscillator band can possess a significant degree of structure. In view of this we anticipate that the dynamic structure factor for the light particles will not be simply a series of structureless peaks.

Before considering the full calculation which includes the mixing of the two types of motion we consider the case when they are well separated in their timescales as in (3.9) and (3.10) and ask how low frequency lattice vibrations effect the oscillator lineshape purely through kinematic or Doppler effects [9]. Let the position of the molecule be $\underline{r}(t)$ and the position of the oscillator bound to it be $\underline{u}(t)$ within the molecular frame. Then $\underline{R} = \underline{r} + \underline{u}$ in the expression (2.1) governing incoherent neutron scattering.

When the parameters are such that the lattice and oscillator bands are well separated, we expect minimal correlation between the two motions. The separation of timescale thus implied leads on the one hand to an extremely narrow oscillator band (essentially an isolated state in the density of states) and on the other hand a separable expression for the correlation function

$$F(k,t) = \langle e^{-i\underset{\sim}{k}\cdot\underset{\sim}{u}(0)} e^{i\underset{\sim}{k}\cdot\underset{\sim}{u}(t)} \rangle_u \cdot \langle e^{-i\underline{k}\cdot\underline{r}(0)} e^{i\underline{k}\cdot\underline{r}(t)} \rangle_r \qquad (4.1)$$

This result can be expressed as a convolution of the two parts labelled L (lattice) and O (oscillator) respectively,

$$S(k,\omega) = \int_{-\infty}^{\infty} d\omega' \, S_L(k,\omega-\omega') S_0(k,\omega') \tag{4.2}$$

Recalling the analysis of section 2 for a single harmonic oscillator and taking the n quanta term in the expansion (2.7) one can immediately perform the convolution in (4.2) to give:

$$S^{(n)}(k,\omega) = S_L(k,\omega-n\omega_0) e^{-2W_0(k)} I_n(y) e^{n\omega_0/2T} \tag{4.3}$$

with y and $2W_0$ defined by (2.8) and (2.9). If in addition we assume that $\omega_0 \gg T$ we get:

$$S^{(n)}(k,\omega) = \frac{1}{n!} S_L(k,\omega-n\omega_0) e^{-2W_0(k)} \left(k^2/2m\omega_0\right)^n \tag{4.4}$$

The line shape is evidently now determined by the lattice function S_L and it is no longer the delta function otherwise implied by the time-scale separation. Egelstaff and Schofield [10] suggest this approach of convolution of two separated effects directly from a consideration of a density of states which includes a band plus one or more split off high frequency modes.

The correlation function $F_L(k,t)$ corresponding to $S_L(k,\omega)$ can be written, with a simple generalisation of (2.6) as

$$F_L(k,t) = e^{-2W_L(k)} \exp\left\{\frac{k^2}{2M}\int \frac{d\omega'}{\omega'} Z(\omega')\left[\coth(\omega'/k_T)\cos\omega' t + i\sin\omega' t\right]\right\} \tag{4.5}$$

where $Z_L(\omega)$ is the density of states in the lattice and M is the mass of the lattice particles. A naive analysis of (4.5) would be to ignore the time dependence, equivalent to taking only the elastic part n=0 of an expansion of $S_L(k,\omega)$. One would then conclude that the contribution of S_L to S is simply exp $(-2W_L(k))$. This lattice Debye-Waller factor would be vanishingly small at the $\underline{k}$ vectors typically employed in a neutron scattering experiment [11,12,13] to investigate the high frequency oscillator behaviour around $\omega = \omega_o$. Despite the appearance of the lattice Debye-Waller factor in the expression for the oscillator line, the experiments referred to above give finite oscillator intensities. This apparent conflict has motivated earlier investigations [9,11]. Intuitively one can picture the motion of the lattice, ie. the molecular contribution, to be frozen over the very short times the neutron interacts with the rapidly moving oscillator. There is consequently no reduction in intensity due to molecular motions. Mathematically if an expansion in phonon number of the type (2.7) corresponding to (4.5) is taken to all orders then the effect of the e^{-2W_L} term is nullified. Placzek [14] recognised that the expansion in phonon number is heavily compensating. Alternatively we can avoid such an expansion and evaluate the exponent in (4.5) for short times $t \ll 1/\theta$, where θ is the upper frequency in the lattice density of states $Z(\omega)$. One gets (from analysis similar to that of (2.15) - (2.19) when examining the impulse approximation for a single oscillator)

$$F_L(k,t) \doteq \exp\left\{-2W_L(k) + k^2/2M \int \frac{d\omega'}{\omega'} Z_L(\omega') \left\{ \coth(\omega'/2T)\left(1-\cos\omega' t\right) + i\omega' t + O(t^3) \right\}\right\} \tag{4.6}$$

The terms independent of t in (4.6) cancel by definition of $W_L(k)$, and there remains

$$F_L(k,t) = \exp\left\{-\tfrac{1}{2}\Gamma^2(T)t^2 + iqt\right\} \tag{4.7}$$

Here the coefficient Γ^2, to become the width function in (4.9) and (4.10) below, is:

$$\Gamma^2(T) = (k^2/2M)\int_0^{\Theta} du\, Z(u)\, u \coth(u/2T)$$

$$\equiv (k^2/M)T \qquad (\text{for } T \gg \Theta) \tag{4.8}$$

where the last result follows from the normalization of $Z(\omega)$. The recoil energy q is simply $k^2/2M$.

These expressions for the width and recoil should be compared with those for the light impurity (3.15) in which it is not the density of states $Z(\omega)$ that appears but a reduced local density of states $Z(\omega)/D(\omega)$ which then gives rise to the striking result (3.19) for q. In section 6 we show how (4.8) for Γ and the result $q = k^2/2M$ alter as a result of the distortion of the density of states and the lack of separation of time-scales when the oscillator band is close to the lattice band.

Proceeding with the case of well separated bands, the corresponding lattice dynamic structure factor is, from (4.7):

$$S_L(k,\omega) = \exp\left\{-(\omega-q)^2/2\Gamma^2(T)\right\} \tag{4.9}$$

The final result for the n^{th} term is then

$$S^{(n)}(k,\omega) = \frac{1}{n!}\left(\frac{k^2}{2m\omega_0}\right)^n \exp\left\{-(\omega-n\omega_0-q)^2/2\Gamma^2(T) \;-2W_0(k)\right\} \tag{4.10}$$

which indicates that the simple oscillator line at $n\omega_0$ is now shifted by recoil to $\omega = n\omega_0 + q$ and broadened to a width $\Gamma(T)$. This is the result of Griffin and Jobic [8].

The analysis above suggests that consideration of the lattice when examining intra molecular modes is vital, shifts and widths being introduced even within a harmonic scheme. Moreover, as experimental resolution continues to improve the structure of lines can also be examined in finer detail. In deriving the Gaussian line shape above one assumes frequencies $\omega \gg \theta$ and thus comments on line structure where $\omega - n\omega_o \lesssim \theta$ will not necessarily be relevant in describing this finer detail now revealed by experiment. We shall therefore present numerical results for S_L.

As the parameters of the model are changed to make the bare oscillator frequency ω_o approach θ , one expects the oscillator band to widen to a width eventually of order θ itself. Moreover, when we examine modes with frequencies around ω_o with increasingly fine resolution, we must consider the effect of band mixing, ie. the removal of the assumption of timescale separation used to achieve the simple forms (4.1) and (4.2). We shall perform an exact normal mode analysis of a model system to illustrate both effects. Equally, as it was necessary to avoid a series representation in the lattice contribution S_L, so will this change in band structure necessitate a full analysis of the oscillator contribution to the dynamic structure factor, $S_0(k,\omega)$. The reason is that the characteristic frequency ω_o is now of the order of the width θ and many quanta effects lead, not to well separated lines, but to a broad envelope. Since we shall be interested in the structure of this envelope on a scale $\sim \omega_o$, an asymptotic analysis of S_0 is inappropriate.

In the next section we present the full analysis of our binary system in some detail since so much analytic progress is possible for a harmonic system, illustrating at the same time the way in which a wide disparity in timescales will lead back to the situation of two independent processes being simply convoluted in the full dynamic structure factor.

5. Binary System: full analysis

Consider a lattice composed of N heavy molecules each of mass M and with a position vector $\underline{x}_\ell$ for the ℓ^{th} molecule. We take these molecules to be harmonically bound to each other so that their equation-of-motion is

$$M \ddot{x}_{\alpha,\ell}(t) = \sum_{\ell'} A_{\alpha\beta}(\underline{\ell}-\underline{\ell}') x_{\beta\ell'}(t) \tag{5.1}$$

where α and β are cartesian labels, ℓ' the six nearest neighbours of ℓ. The dynamical matrix $\underline{A}$ describes a simple cubic system with waves such that:

$$A_x(\underline{x})/M = A_y(\underline{y})/M = A_z(\underline{z})/M = \omega_t^2/4 \tag{5.2a}$$

$$A_x(\underline{y} \text{ or } \underline{z})/M = \text{permutations} = \omega_t^2/4 \tag{5.2b}$$

and where the quantities in (5.2) are the diagonal elements of $A_{\alpha\beta}(\ell)$

$$A_{\alpha\beta}(\underline{\ell}) = \begin{pmatrix} A_x(\underline{\ell}) & 0 & 0 \\ 0 & A_y(\underline{\ell}) & 0 \\ 0 & 0 & A_z(\underline{\ell}) \end{pmatrix} \tag{5.3}$$

The special assumptions in equations (5.2) and (5.3) as to the character of the dynamical matrix are somewhat unrealistic but result in calculational simplicity in what follows. Most importantly the density of states we derive from this dynamical system will be seen to resemble those of real systems [15, 16]. Features from the lattice density of states turn out to dominate the fine structure of the oscillator dynamical structure factor.

Fourier transforming to $\underline{q}$ space to give

$$x_\beta(q) = \sqrt{M/N} \sum_{\underline{\ell}} e^{i q \cdot \underline{\ell}} x_\beta(\underline{\ell}) \tag{5.4}$$

yields the usual N eigen modes with frequencies $\Omega_\alpha(\underline{q})$ given by

$$\Omega_\alpha^2(q) = \omega_\ell^2 \sin^2(q_\alpha a/2) + \omega_t^2 \left\{ \sin^2(q_\beta a/2) + \sin^2(q_\gamma a/2) \right\} \tag{5.5}$$

All normal vibrations are along a principal axis. When q is, for example, in the α direction we have a purely longitudinal wave for the eigen mode with frequency ω_ℓ. When q is in either of the other two directions β or γ we have a purely transverse wave of frequency ω_t.

If now we consider a lighter mass m to be isotropically bound within each molecule and to have a coordinate $\underline{y}_\ell$ then the coupled equations-of-motion are (Fourier transforming in time to give frequencies ω_α):

$$\omega_\alpha^2 x_\alpha(q) = -\Omega_\alpha^2 x_\alpha(q) + (K/M) x_\alpha(q) - (K/\sqrt{Mm})\, y_\alpha(q)$$

$$\omega_\alpha^2 y_\alpha(q) = \omega_0^2 y_\alpha(q) - (K/\sqrt{Mm})\, x_\alpha(q) \tag{5.6}$$

The stiffness of binding is K for the mass m. The coordinate $\underline{y}$ has also been Fourier transformed according to

$$y_\alpha(q) = \sqrt{m/N} \sum_{\underline{\ell}} e^{i q \cdot \underline{\ell}} y_\alpha(\underline{\ell}) \tag{5.7}$$

The frequency ω_o in (5.6) is the bare oscillator frequency defined by

$$\omega_o^2 = k/m \tag{5.8a}$$

It is convenient to introduce three parameters for the model

$$\eta = \omega_t^2/\omega_l^2 \tag{5.8b}$$

$$\gamma^2 = k/\sqrt{Mm} \equiv \omega_o^2/\sqrt{M} \tag{5.8c}$$

and

$$\overline{\omega}^2 = k\left(\frac{1}{M}+\frac{1}{m}\right) = \omega_o^2 + k/M \tag{5.8d}$$

From the comments following (5.5) we see that η expresses the ratio of the squares of speeds of sound in the lattice when we have purely longitudinal or transverse waves.

The maximum frequency, θ, in the lattice when unperturbed by the oscillators is given in terms of the characteristic lattice frequency ω_ℓ by the relation

$$\Theta^2 = (2\eta+1)\omega_\ell^2 \tag{5.8e}$$

The coupled equations of motion (5.6) now yield (for each α, which we omit for ease of notation) the eigen equations

$$(\Omega_q^2 + k/m)x(q) - \omega^2 x(q) - \gamma^4 y(q) = 0$$

$$-\gamma^2 x(q) + \omega_0^2 y(q) - \omega^2 y(q) = 0 \qquad (5.9)$$

with eigen frequencies $\omega_\pm$

$$\omega_\pm^2(q) = \frac{1}{2}\left\{\omega^2 + \Omega_q^2 \pm \sqrt{(\omega^2+\Omega_q^2)^2 - 4\omega_0^2\Omega_q^2}\right\} \qquad (5.10)$$

The + solution evidently yields oscillator-like motions with eigen vectors $U_+(q)$

$$U_+(q) = \frac{1}{\sqrt{1+\tau_+^2}}\left\{x(q) - \tau_+ y(q)\right\}$$

$$\tau_+ = \gamma^2/(\omega_+^2 - \omega_0^2) \qquad (5.11)$$

The - solution yields a phonon-like band with eigen vectors $U_-(q)$:

$$U_-(q) = \frac{1}{\sqrt{1+\tau_-^2}}\left\{x(q) + \tau_- y(q)\right\}$$

$$\tau_- = \gamma^2/(\omega_0^2 - \omega_-^2) \qquad (5.12)$$

The oscillator coordinate y_q now becomes, in terms of eigen vectors $U_\pm$ of the problem:

$$y(q) = -\frac{\tau_+}{\sqrt{1+\tau_+^2}} U_+(q) + \frac{\tau_-}{\sqrt{1+\tau_-^2}} U_-(q) \tag{5.13}$$

The incoherent dynamic structure factor for a light particle is

$$S(k,\omega) = \frac{1}{2\pi}\int_{-\infty}^{+\infty} dt\, e^{-i\omega t} \left\langle e^{-i\underset{\sim}{k}\cdot \underset{\sim}{y}(0)}\, e^{+i\underset{\sim}{k}\cdot \underset{\sim}{y}(t)} \right\rangle$$

which, from the orthogonality of the normal modes, can rigorously be written

$$\frac{1}{2\pi}\int dt\, e^{-i\omega t} \left\langle e^{-i\underset{\sim}{k}\cdot \frac{\tau_+}{\sqrt{1+\tau_+^2}} \underset{\sim}{U}_+(0)}\, e^{-i\underset{\sim}{k}\cdot \frac{\tau_+}{\sqrt{1+\tau_+^2}} \underset{\sim}{U}_+(t)} \right\rangle_{\underset{\sim}{U}_+} \cdot$$

$$\cdot \left\langle e^{-i\underset{\sim}{k}\cdot \frac{\tau_-}{\sqrt{1+\tau_-^2}} \underset{\sim}{U}_-(0)}\, e^{i\underset{\sim}{k}\cdot \frac{\tau_-}{\sqrt{1+\tau_-^2}} \underset{\sim}{U}_-(t)} \right\rangle_{\underset{\sim}{U}_-} \tag{5.14}$$

Now, since we have the problem expressed in terms of eigen vectors U_+ and U_- the quantization is trivial and the ensemble average can be evaluated in the conventional way [17]. The question of polarizations is also trivial in this simple model system. Thus $S(k,\omega)$ is again a convolution

$$S(k,\omega) = \int d\omega'\, S_-(k,\omega-\omega')\, S_+(k,\omega') \tag{5.15}$$

where

$$S_{\pm}(k,\omega) = \frac{1}{2\pi}\int dt\, e^{-i\omega t} F_{\pm}(k,t) \tag{5.16a}$$

and

$$F_{\pm}(k,t) = e^{-2W_{\pm}(k,t=0)}\, e^{2W_{\pm}(k,t)} \tag{5.16b}$$

and where

$$W_{\pm}(k,t) = \left(k^2/4m\right)\int_{-\infty}^{+\infty} \frac{du}{u} Z_{\pm}(u) C(u) \left\{G(u,t) - 1\right\} \tag{5.16c}$$

Equation (5.16c) is the usual expression, with a density of states $Z_{\pm}(\omega)$ for each band, but with the additional factor $C(\omega)$ arising from the normal mode separation (see equation 5.13)

$$C(\omega) = \frac{\tau_{\pm}^2}{1+\tau_{\pm}^2} = \frac{\gamma^4}{(\omega^2-\omega_0^2)^2+\gamma^4} \tag{5.17}$$

The case where there is time-scale separation between the two solutions is be achieved for instance by letting the mass ratio m/M get small. In that case one has the values for $C(\omega)$:

$$C(\omega) \longrightarrow m/M \tag{5.18a}$$

for $\omega \leq \theta \ll \omega_0$, ie. in the lower band; and

$$C(\omega) \longrightarrow 1 \tag{5.18b}$$

for $\omega \sim \omega_0$, ie. in the upper band.

The expressions (5.16c) for $W_{\pm}(k,t)$ then return to their conventional values for phonons and oscillators used in the analysis of section 4 where this separation was assumed.

For the case where m/M is not small or, more generally, ω_o/θ is not extremely large both the oscillator and lattice bands contributed equally to the structure factor. We proceed by calculating the density of states $Z_{\pm}(\omega)$ within this model. This being done, $W_{\pm}(k,t)$ can be evaluated and thence S_L and S_O, and S by convolution.

The density of states $Z_{\pm}(\omega)$ is given by

$$Z_{\pm}(\omega) = \left(\frac{a}{2\pi}\right)^3 \int_{BZ} d\underline{q}\, \delta\left(\omega - \omega_{\pm}(\underline{q})\right) \qquad (5.19)$$

where the integral over modes $\underline{q}$ is over the Brillouin zone and the mode label α is suppressed since the results are independent of α in this simple cubic system. We recall that, with the definitions (5.8), we have for Ω (which expresses the dispersion in the normal mode frequencies (5.10)).

$$\Omega_Z^2(q) = \omega_\ell^2 \left\{ \sin^2(q_z a/2) + \eta\left[\sin^2(q_x a/2) + \sin^2(q_y a/2)\right] \right\}$$

This suggests the natural units of $Z(\omega)$ are $1/\omega_\ell$. Hence-forth we shall reduce all frequencies by the characteristic frequency of the lattice, ω_ℓ.

$$Z(\omega) \longrightarrow \frac{1}{\omega_\ell} Z(\omega) \qquad (5.20)$$

where the ω on the right hand-side is the reduced form. The actual calculation of $Z(\omega)$ can mostly be done analytically by judicious changes of variable and this is shown in the appendix.

As was clear from the solution for the eigen frequencies there are two bands, a low frequency lattice band and an oscillator band starting at $\omega=\bar{\omega}$. When the bands are well separated, that is $\bar{\omega} >> \sqrt{2\eta+1}$ the upper band tends

to $Z_+(\omega) = \delta(\omega-\omega_0)$ with $\overline{\omega} \approx \omega_0$. A limit where this occurs is when the masses are disparate, that is m/M 1. At the other extreme where $\omega_0 \approx (2\eta+1)^{\frac{1}{2}}$, the top of the lattice band is pushed down below the value $(2\eta+1)^{\frac{1}{2}}$ and the bottom of the oscillator band $\overline{\omega}$ is pushed away from ω_0. The upper band is wide, of the order of θ and mirrors the structure of the lower band. An example of this extreme is given in figure (2) for the case $\eta=1$, $\alpha(\equiv\omega^2/\omega_\ell^2)=2$ and M/m = 25.

In what follows we shall use reduced wavevectors, temperatures and times in terms of ω_ℓ:

$$Q^2 = \hbar^2 k^2 / 2m\hbar\omega_\ell$$
$$T^* = k_B T / \hbar\omega_\ell \qquad (5.21)$$
$$\tau = \omega_\ell t$$

We display $\hbar$ and k_B to illustrate the relation to experimental values k, T, t. Examples are given in section 6.

The final expressions for the $S_\pm(Q,\omega)$ are then

$$S_\pm(Q,\omega) = \frac{1}{2\pi\omega_\ell}\int_{-\infty}^{+\infty} d\tau\, e^{-i\omega\tau + 2W_\pm(Q,\tau)}$$

with (5.22)

$$W_\pm(Q,\tau) = \frac{Q^2}{2}\int_0^\infty \frac{du}{u} Z_\pm(u)\,C(u)\,G(u)$$

6. Binary System; numerical results

The evaluation of the dynamic structure factor involves the Fourier transformation (5.16a) of the correlation function F(k,t). Since the factor G(ω,t) in the exponent (5.16c) of F(k,t) is composed of trigonometric functions, Fourier transformation is also suggested there. When $k^2/4m$ is large usual series methods to render such transforms trivial fail and we turn, because of the very rapid oscillatory behaviour, to the

fast Fourier transform. Since this numerical technique employs a periodic representation of the function great care has to be taken to insure that periodic repetition of features and the effect of truncation do not get confused with complex multiquanta effects. We now proceed by dividing our discussion into two parts, the cases of (i) well separated and (ii) close bands.

(i) We report on the effect of the lattice-like modes on the oscillator lines when the bands are well separated, that is when the oscillator frequency ω_o is well above the maximum of the phonon band with the consequence that the oscillator lines are intrinsically narrow. All broadening is due only to the "kinetic"effect of the lower band. In this case we return to the analysis of (4.3) and seek the effect of convoluting the lattice part, S_-, with the oscillator line; in other words, what is the additional structure to the line aside from the usual $I_n(y)\exp(-2W_o(k) + nh\omega_o/2K_BT)$ weighting factor?

The structure factor of the Gaussian form (4.9) in the high Q limit requires a width Γ as in (4.8) which is now,

$$\Gamma^2(T) = \Phi^2 \int_0^{\omega_{max}} d\omega \, Z_-(\omega) C(\omega) \omega \coth(\omega/2T^*) \tag{6.1}$$

while the free-particle recoil $q = k^2/2M$ is replaced by

$$q = \Phi^2 \int_0^{\omega_{max}} d\omega \, Z_-(\omega) C(\omega) \tag{6.2}$$

where ω_{max} is the maximum frequency of the lower band and, because of the full normal mode separation, the factor $C(\omega)$ is not constant. In the limit $m \ll M$ the $C(\omega) \to (m/M)$ and $q \to Q^2 m/M \equiv k^2/2M$, which is the free-particle recoil in reduced units. We deduce from (6.2) that,

$$q \geq Q^2 m/M \tag{6.3}$$

since one has $C(\omega) \geq m/(M+m)$. Likewise, when $2T^* \gg \omega_{max}$ then

$$\Gamma^2(T) \rightarrow 2T^*Q^2 \int_0^{\omega_{max}} d\omega \, Z_-(\omega) C(\omega)$$

$$\rightarrow T^* k^2/M$$

for $m \ll M$ (in units of ω_{ℓ}^2). In general we have the inequality:

$$\Gamma^2(T) \gtrsim 2T^*Q^2 \tag{6.4}$$

In fact we shall see that widths Γ and recoils q, even in cases to be considered below where bands appear well separated, are greatly enhanced above the limiting values indicated in the inequalities (6.3) and (6.4).

A further important preliminary to presenting our results is that there is an elastic, recoiless component to the structure factor (5.22). As $\tau \to \infty$ the function $W_-(Q,\tau) \to -2W(Q)$, where the latter is the conventional exponent of the Debye-Waller factor. Thus the Fourier transformation (5.22) also yields an elastic component to S_- of $\exp(-2W_-(Q)).\delta(\omega)$ which we remove by evaluating

$$\hat{S}_-(Q,\omega) = \frac{1}{2\pi\omega_\ell} \int_{-\infty}^{\infty} d\tau e^{-i\omega\tau} \left\{ e^{2W_-(Q,\tau)} - e^{-2W_-(Q)} \right\} \tag{6.5}$$

Hereafter the tilde will denote quantities with the delta function component subtracted out. One must therefore remember in examining the line shapes obtained by convoluting $\tilde{S}_-(Q,\omega)$ that a weight $\exp(-2W(Q))$ resides in the sharp component, not shown. This is a very small contribution at the high Q vectors normally chosen to examine the oscillators, but we make this proviso in order to show how these broad lines eventually go over to the sharp lines observed at Q and $T^* \to 0$.

A consequence of this is that the normalization of the equivalent Gaussian structure factor with width function Γ is

$$\left(1-e^{-2W_{-}(Q)}\right)\left(2\pi\Gamma^{2}\right)^{-1/2} \tag{6.6}$$

and not the value appearing in (2.19).

For the case of η=1, M/m=25, and $\alpha(\equiv \overline{\omega}^{\,2}/\omega_{\ell}^{2}) = 5$ one has bands reasonably well separated. A measure of this criterion is seen in the band structure which shows that the top of the lattice band is at $\omega = .957\theta$ (not much depressed from θ by the influence of the other band) and that the upper band (starting at $\omega = \overline{\omega} = 1.291\theta$) only has a width of $.033\theta$. We now proceed in figures (3) to (6) to examine the dynamical structure resulting from these bands. The contribution $S^{(n)}(Q,\omega)$ corresponding to (4.3) is

$$S^{(n)}(Q,\omega) = I_{n}(y)\, e^{n\omega_{0}/2T^{*}-2W_{+}(Q)}\, S_{-}(Q,\omega-n\omega_{0}) \tag{6.7}$$

We plot in figures (3) - (6) the part $\hat{S}_{-}$ of of S_{-} in (6.7) which in neutron scattering represents the line shape for scattering from the light particle in the binary system. Figure (3) illustrates the line shape (neglecting the oscillator band width) for neutron scattering with a scattering vector Q = 2 and at two temperatures T^{*} = 1 and T^{*} = 2. The essential line-shape is that due to single lattice excitations, or phonon, processes and mirrors the density of states $Z_{-}(\omega)$. Up scattering processes are seen to obey the detailed balance condition. Already there is, crudely speaking, more structure corresponding to two phonon processes around $\omega = n\omega_{0} + 2.4$. The effect of doubling the temperature to T^{*} = 2 shows the inevitable increase in up scattering and the decrease of the Debye-Waller factor (DWF) $\exp(-2W_{-}(Q))$ from .553 to .332. Remembering that the area under $\hat{S}_{-}(Q,\omega)$ presented here is (1-DWF) and that the weight of the unbroadened line at $\omega = n\omega_{0}$ is the DWF, it is clear that raising the temperature markedly

increases the shifted component. It is not immediately clear what fraction of the total intensity must be in the broadened component before it becomes experimentally observable.

Before examining the effect of increasing the momentum transfer Q it is instructive to estimate, for a typical material, what k and T these Q and T^* correspond to. Taking the example of the hexamethylenetetramine (HMT) lattice modes we deduce, from the work of Dolling and Powell [15], the values $\eta = .5$, $\upsilon_{max} \approx 2.4 \times 10^{12}$hz. With an assumption that the bands are well separated, we have $\upsilon_{\ell} = \upsilon_{max}/\sqrt{2} = 1.7 \times 10^{12}$hz (the υ's are the frequencies corresponding to the ω's), giving the relations

$$\begin{aligned} k &= 1.822Q \quad (k \text{ in } \text{Å}^{-1}) \\ T &= 85T^* \quad (T \text{ in } {}^{o}K) \\ E &= 7.0\omega \quad (E, \text{ neutron energy transfer, in meV}) \end{aligned} \tag{6.8}.$$

In other words the results above would be, in case of HMT, for $k = 3.65\text{Å}^{-1}$ and temperatures of $85^{o}K$ and $170^{o}K$.

We now examine the effect of increasing Q. Figure (4) shows $\hat{S}_{-}(Q,\omega)$ for Q=4. Multiphonon effects now dominate the line shape but much structure is still evident, both in the region $\omega = n\omega_o$ to $n\omega_o \pm \theta$ mirroring the density of states, and in the region beyond this where successive multiphonon humps in $\hat{S}_{-}(Q,\omega)$ are evident. The Debye-Waller factor is now .012 indicating that essentially all the weight resides in the figure as shown and little in the unshifted line. With currently available resolutions (often a small fraction of typical values of θ) it is clear that even at such Q values (equivalent to 7.3Å^{-1} in the example of HMT) a structure consisting of four peaks and perhaps shoulders would be seen. We emphasise that this result has been achieved within an harmonic approximation and assuming no intrinsic structure to the oscillator function. A cautionary note must therefore be sounded about a too rapid recourse to more complicated possible explanations of observations of apparently split peaks or fine structure when inelastically scattering from internal modes of molecules or from other oscillators in a lattice.

The same remarks are applicable to the scattering off light mass impurities in a lattice. An underlying lattice density of states resembling the one we have chosen here and the use of a Q and T^* sufficient to cause some degree of multiphonon effects in $\tilde{S}_-$ will be sufficient to give such features as an apparent asymmetric splitting as evidenced in a dynamical structure factor of the form in figure (4).

Proceeding to still higher values of Q (Q=5,6)with T^* fixed at $T^*=2$ we see in figures (5) and (6) the smoothing out of phonon effects to give an envelope that is evidently tending to a Gaussian shape. The Debye-Waller factors $\exp(-2W_-(Q))$ for the lattice are now vanishingly small and essentially all of the S_L contribution to $S^{(n)}$ in (6.7) resides in the part of S_- broadened and shifted, that is $\tilde{S}_-$, defined in (6.5) and plotted in the figures. It remains for the case of separated bands, to consider the transition to the impulse approximation for $S_-(Q,\omega)$, that is, the Gaussian form with width Γ and recoil q from equations (6.1) and (6.2). We recall that these expressions differ from the simple expressions (4.8) for Γ and $q=Q^2$ by the appearance of the coefficient $C(\omega)$ from the lack of timescale separation (ie. from the full normal mode analysis). In fact the former relations obtain in the limit of uncorrelated lattice and oscillator motion by the use of the limiting form $C(\omega) = m/M$.

For the temperature $T^*=2$ relating to figures (4), (5) and (6) the values of Γ/Q and q/Q^2 are (with the values obtained from C=m/M in parentheses) .573 (.405) and .0796 (.0399). Thus ignoring the problem of time-scale separation leads to errors of a factor of 2 in the apparent recoil energy and of 1.4 in the width for this particular choice of band parameters. It is to be emphasised that this is even for a case where the frequencies ω_ℓ (characteristic of the lattice) and ω_o (for the internal mode) are sufficiently different that the oscillator line has a negligible intrinsic width. Comparison between the Gaussians (the broken lines in the figures) with these Γ and q and the structure factors they are supposed to represent shows that the characteristic widths are an excellent representation as Q increases, that the shifts tend to be slightly larger and that the detailed structure around $\omega = n\omega_o$ to $n\omega_o + \theta$ is completely wrong, as indeed consideration of the validity of the expansion (4.6) shows it must be.

(ii) We now report on the case where the lattice and oscillator bands are not well separated. In fact we shall take a case where they are of equal widths, that is when the proximity of the oscillator band to the lattice band has produced an intrinsic width to the former band equal to that of the latter. This is achieved for example by use of the extreme parameters $\alpha = 0.9$, $M/m = 5$ and $\eta = 1$.

The convolution of S_+ and S_- in the first case was essentially trivial since S_+ was sharp (at $n\omega_o$) and the entire structure of the resulting line (centred near $n\omega_o$) was due to S_-. We now require a numerical convolution of the two parts. Figure (7) shows $\tilde{S}(Q,\omega)$ the tilde again indicating the removal of the delta function components, at low Q (0.1) and T^* (0.1) which, under these extreme conditions, is essentially $C(\omega)[Z_-(\omega) + Z_+(\omega)]/\omega$. Thus figure (7) closely mirrors the densities of states Z_- and Z_+. Already we see that, although we are scattering from the lighter masses (with characteristic frequencies around 1.65) we are also sensitive to motions when the scattering centres move with the lattice (the lower frequency motions around 0.75). In fact inspection of the figure shows that the $C(\omega)$ factor from the normal mode analysis is such that the motions around $\omega = .75$ appear with the greater weight, in contrast to the situation of figures (3) - (6) where the m/M factor from $C(\omega)$ and the narrowness of the oscillator band make the contribution to the light mass motion from the modes of the upper band much greater than from the lower band. We refer to the resolution of the oscillator coordinate into lattice and oscillator components in expressions such as (5.14) and (5.16). Higher Q(1.0) and $T^*(1.0)$ as shown in figure (8) show multi-quanta effects (at $\omega \approx 2.5$ and 3.5 for example), up-scattering (at $\omega > 0$) and an increased relative magnitude of the upper band fundamental at $\omega \sim 1.65$ compared with the lower band contribution. The Debye-Waller factor, $\exp(-2W_-(Q)-2W_+(Q))$, is 0.0532 indicating that 95% of the total intensity in $S(Q,\omega)$ is in the figure, that is, in $\tilde{S}(Q,\omega)$ and 5% is in the inelastic line not shown. The spectrum shows a central broadened line which arises out of the contribution roughly speaking of $C(\omega)Z_-(\omega)\coth(\omega/2T)/\omega$ as $\omega \to 0$ and for T large. Inspection of this $\tilde{S}(Q,\omega)$ shows the great possibility of ambiguity in interpreting the spectrum as a series of slightly broadened oscillator lines. This simple harmonic analysis shows that the lattice band is responsible for every

second line and that the intrinsic oscillator lineshape is not narrow or simple, even before the kinematic effects of convolution with the lower band are considered.

We also remark on the fact that for this choice of band parameters the multi-quanta effects appear more pronounced at a relatively lower Q than was found for the case of a narrow oscillator band. One must note that the Q is a wave vector reduced by the characteristic lattice frequency ω_ℓ. The lattice part S_L can be seen in figure (7) to have its peak at a frequency less than ω_ℓ (around .8 in units of ω_ℓ) rather than above it, as in the example leading to figure (3); Q^2 is effectively greater as a result. Another contributory factor in the structure of S_L is the now much greater values of $C(\omega)$ in the expression for S_L which also can be thought of as enhancing the effective value of Q^2. Care must therefore be taken in deciding, when comparing with experiment, what reduced Q is equivalent to the actual wavevector k. The intrinsic width of the oscillator band, seen at low k and T, is evidently the guide for finding the correct connection between the characteristic frequency of the lattice band and the reduced wavevector Q. In consequence the scaling (6.8) for separated bands where $\omega_\ell = \omega_{max}/\sqrt{2\eta+1}$ would now be in error. Q and T^* for close bands correspond to larger k and T than before because ω_ℓ, deduced from the observed ω_{max}, is larger than the above relationship suggests.

If now the temperature is doubled to the value $T^* = 2$ in figure (9) with wavevector remaining at the value $Q = 1$, the effect is to reduce the peak intensities considerably for lower energy transfer and to increase the peak values at higher energy transfer. The background level remains roughly the same. The Debye-Waller factor here, and in the examples to follow, is essentially zero.

Keeping the temperature fixed at $T^* = 2$ we examine the effect of varying momentum transfer by increasing Q from the value $Q = 1$ (figure (9)) to $Q = 1.5$ (figure (10)) and $Q = 2$ (figure (11)). The background level is not greatly effected but there is a rapid fall in the peak intensities so that at $Q = 2$ peaks are only (weakly) resolvable around the centre of the shifted background to $S(Q, \omega)$. The background takes on a shifted Gausian character with widths of 2.729, 3.638 and shifts of 1.838, 3.267 for $Q = 1.5$ and $Q = 2.0$, respectively, and are shown as broken lines in the figures. The Gaussian approximation cannot reproduce the detailed

structure surviving from the lattice that still exists around the centre of the envelope. The figures indicate however that as Q increases there is a rapid transition toward the Gaussian approximate structure factor.

7. Summary

In this paper we have analysed the dynamic structure factor for an oscillator - either a light impurity in a harmonic lattice or a binary system of light and heavy masses forming a harmonic lattice. These are models of systems frequently investigated by neutron scattering, namely impurities such as hydrogen in metallic lattices and the motion of light entities in large molecules, themselves bound as part of molecular solid.

Many problems immediately arise from the existence of a surrounding lattice. For example, the Debye-Waller factor from the lattice component of motion becomes vanishingly small at the wavevector k inevitably [13] encountered in highly inelastic experiments. This lattice component, since it is convoluted with the oscillator contribution, would appear to have a nugatory effect.

In fact the elastic part of the lattice contribution (weighted by this small Debye-Waller factor) is then replaced with a shifted and broadened contribution which, in the simplest case of an intrinsically narrow oscillator line at ω_o, results in a shifted and broadened line near ω_o after the necessary convolution is done.

We present asymptotic results for this line shape and recoil for the case of the isolated light mass impurity and detailed numerical results for the binary system. Both are the fruits of exact solutions which are possible in such simple harmonic systems. The conclusions are that the contributions from the lattice are <u>not</u> to produce a small Debye-Waller factor, but result in a line with a finite intensity, albeit shifted and broadened. The shift in intensity from the central to the broadened part of the resultant oscillator line is easy to follow. A further conclusion is made in the binary system: in the transition region from the lowest attainable k values to values around 8Å^{-1} there is significant structure in the oscillator line surviving from the underlying lattice vibrational density of states (see figure (4)). At very high k values one would expect

a Gaussian form to $S(k,\omega)$ which is indeed observed in the wings of figure (4). However, our conclusion is that the remaining structure is directly explicable in terms of our simple harmonic model. One must be extremely cautious, when interpreting such "split" peaks, not to introduce more complicated explanations (more than one site, anharmonicity . . .) before eliminating the present cause.

The Gaussian approximation to $S(k,\omega)$, alluded to above, has been discussed previously [9,10]. We derive it in several contexts in this paper and criticize its validity. It does not reproduce the detailed structure of the above examples because it relies on an expansion invalid at frequencies in the range of order of $\pm\theta$ (a characteristic lattice frequency) around the central frequency of the Gaussian. As we point out, with currently available resolutions, this can be a limitation. The anticipation of such a featureless form of $S(k,\omega)$ would lead to erroneous conclusions if features as in figure (4) were to be observed.

The other main problem arising from the lattice environment is that strictly speaking a full normal mode analysis of the binary system must be carried out. We do this and find that, even for oscillators which are apparently well separated in frequency from the lattice motions, appreciable differences occur between the full analysis and an analysis assuming that the separation is complete. A direct consequence is that the effective widths and shifts characterising the Gaussian approximation to $S(k,\omega)$ are inaccurate (by a factor of 2 for the example we present in section 6). In general terms however, the Gaussian approximation is seen to accurately mirror the actual $S(k,\omega)$ when k and T (temperature) are sufficiently great that multiphonon processes dominate.

The importance of relative timescales of lattice and oscillator motions is underlined when we examine an example where the oscillator frequency is close to θ. Although we are observing the dynamic structure factor of the oscillator our results show that there are now strong contributions to $S(k,\omega)$ at the lattice characteristic frequency (and its harmonics) resulting from the lack of timescale separation in the coupling. Another important consequence is that the oscillator line can no longer be sharp, an intrinsic width arising out of the band mixing when the two bands are close. The results of the above two effects is a series of broad lines on top of a broad background as displayed in figures (8 - 11).

In conclusion we have demonstrated a great richness of effects to be encountered in inelastic scattering from systems of great interest, even within simple models with harmonic couplings. The complexity encountered in real systems must be interpreted in light of what is already generated by simple systems.

Acknowledgements

We are grateful to Sir Rudolf Peierls, and Drs J Penfold and J Tomkinson for stimulating discussions and a critical reading of the manuscript. The numerical calculation of the density of states was checked using an integration program supplied by Dr J F Cooke, and we are very grateful for his considerable efforts on our behalf.

APPENDIX

The density of states Z(ω)

In the expression (5.19) for Z change variables to y=q(a/2). Then

$$Z_{\pm} = 8/(\omega_l \pi^3) \int_0^{\pi/2} dy\, \delta(\omega - \omega_{\pm}(y)) \qquad (I.1)$$

where at the same time the transition to the dimensionless variable ω/ω_l has been made. A re-arrangement of the dispersion relation (5.10) leads to:

$$\varkappa \sin^2 y_z + \eta(\varkappa \sin^2 y_x + \varkappa \sin^2 y_y) = \frac{\omega^2(\omega^2 - \bar{\omega}^2)}{\omega^2 - \omega_0^2} = \xi(\omega) \qquad (I.2)$$

A further change of variable then suggests itself:

$$S_\alpha = \varkappa \sin^2 y_\alpha$$

whereupon Z(ω) becomes:

$$Z(\omega) = (\pi^3 \omega_l)^{-1} \int_0^1 \prod_\alpha \frac{dS_\alpha}{\sqrt{S_\alpha - S_\alpha^2}}\, \delta(\omega - \omega(\underline{S})) \qquad (I.3)$$

$$= (\pi^3 \omega_l)^{-1} \int_\omega \frac{d\Lambda_\omega}{\prod_\alpha (S_\alpha - S_\alpha^2)^{1/2}} \frac{1}{|\nabla_{\underline{S}} \omega(\underline{S})|_\omega} \qquad (I.4)$$

where $d\Lambda_\omega$ is an element of the surface of constant ω in s-space. The relation (I.2), now in the form

$$S_z + \eta(S_x + S_y) = \xi(\omega) \tag{I.5}$$

shows that the surface of constant ω is simply a plane in s-space allowing the integral (I.4) to be completed in a simple manner. The gradient term is

$$\left|\nabla_s \omega(\underline{S})\right| = \frac{\sqrt{2\eta^2+1}}{2\omega} \frac{(\omega^2-\omega_0^2)^2}{(\omega^2-\omega_0^2)^2+\gamma^4} \tag{I.6}$$

The plane of constant frequency can be parametrized by two coordinates λ and μ by changing variables so that

$$\underline{S}(\lambda,\mu) = \xi(\omega)(0,0,1) + \lambda(-1,1,0) + \mu(1,1,-2\eta) \tag{I.7}$$

whence the density of states $Z(\omega)$ (in units of $1/\omega_\ell$) becomes

$$Z(\omega) = \left(\frac{4\omega}{\pi^3}\right)\frac{(\omega^2-\omega_0^2)^2+\gamma^4}{(\omega^2-\omega_0^2)^2}\int \frac{d\mu}{(\xi(\omega)-2\eta\mu)^{1/2}(1-\xi(\omega)+2\eta\mu)^{1/2}} \cdot$$

$$\cdot\int \frac{d\lambda}{(\mu^2-\gamma^2)^{1/2}((\mu-1)^2-\gamma^2)^{1/2}} \tag{I.8}$$

The limits of the λ integration are $\int_0^{\mu} d\lambda$ or $\int_0^{1-\mu} d\lambda$ for $\mu < \frac{1}{2}$ or $> \frac{1}{2}$ respectively. For $\int d\mu$ the limits are determined by the value of $\xi(\omega)$, ie. of ω and are illustrated in figure (12). The $\int d\lambda$ then yields complete elliptic functions of the first kind, κ, that is

$$H(\mu) = \int d\lambda (\text{----}) = \frac{1}{1-\mu} K\left(\frac{\mu}{1-\mu}\right) \qquad \mu < \tfrac{1}{2}$$

$$= \frac{1}{\mu} K\left(\frac{1-\mu}{\mu}\right) \qquad \mu > \tfrac{1}{2}$$

The remaining μ integral is a simple numerical integral

$$Z(\omega) = \left(\frac{4\omega}{\pi^3}\right)\left[\frac{(\omega^2-\omega_0^2)^2+\gamma^4}{(\omega^2-\omega_0^2)^2}\right]\int \frac{d\mu\, H(\mu)}{(\xi(\omega)-2\eta\mu)^{1/2}(1-\xi(\omega)+2\eta\mu)^{1/2}} \qquad \text{(I.9)}$$

References

[1] Howard J and Waddington T C: Advances in Infrared and Raman Spectroscopy, Chapter 3, Vol.7. Clark R J H and Hester R E (eds). Heyden and Sons, 1980.

[2] Springer T: Hydrogen in Metals I, Chapter 4. Alefeld G and Völkl J (eds). Berlin: Springer-Verlag, 1978.

[3] Severin H, Wilson S K P, Wicke E and Ross D K: to be published.

[4] Squires G L: Thermal Neutron Scattering. Cambridge: University Press, 1978.

[5] Lovesey S W: Condensed Matter Physics, Dynamic Correlations. Massachusetts: Benjamin, 1980.

[6] Rahman A, Singwi K S and Sjölander A: Phys. Rev. 126, 986 (1962).

[7] Bloch F: Z Phys. 74, 295 (1932).

[8] Maradudin A A, Flinn P A and Ruby S L: Phys. Rev. 126, 9 (1962).

[9] Griffin A and Jobic H: J. Chem. Phys. 75, 5940 (1981).

[10] Egelstaff P A and Schofield P: Nucl. Sci. Eng. 12, 260 (1962).

[11] Jobic H, Ghosh R E and Rencuprez A: J Chem. Phys. 75, 4025 (1981).

[12] Vibrational spectroscopy on a pulsed neutron source employs relatively high momentum transfers, for example:
Boland B C, Mildner D F R, Stirling G C, Bunce L J, Sinclair R N and Windsor C G: Nucl. Inst. Meth. 154, 349 (1978).

[13] The limitation to working at relatively high momentum transfer $k(> .5\text{Å}^{-1})$ when performing neutron spectroscopy is analysed, for example:
Brugger R M, Strong K A and Grant D M: p.323 Neutron Inelastic Scattering, Vol.II. Vienna: International Atomic Energy Agency, 1968.

[14] Placzek G: Phys. Rev. 86 377 (1952), 93 895 (1954), 105 1240 (1957).

[15] Dolling G and Powell B M: Proc. Roy. Soc. Lond. A319, 209 (1970).

[16] Bilz H and Kress W: Phonon Dispersion relations in Insulators. Berlin: Springer-Verlag, 1979).

[17] Marshall W and Lovesey S W: Theory of Thermal Neutron Scattering. Oxford: Clarendon Press, 1971.

Figure Captions

Figure 1

The amplitude $h(x)$ of the light mass impurity mode against reduced frequency x. $h(x)$ is introduced in equation (3.6a) for the correlation function.

Figure 2

The densities of states $Z_-(\omega)$ and $Z_+(\omega)$ for a binary system. The parameters of the bands are $\eta=1$, $M/m=25$ and $\alpha=2$ (defined in equations (5.8)). This is a case where the upper band is sufficiently close to the lower that there is significant band mixing and intrinsic width to the oscillator band. The frequency ω is reduced by the characteristic frequency ω_ℓ of the lattice.

Figure 3

The dynamical structure factor $\hat{S}_-(Q,\omega)$ against energy transfer (ω). $\hat{S}_-(Q,\omega)$ is plotted for two temperatures $T^*=1,2$ at a fixed scattering vector $Q=2$. The Debye-Waller factors are .553 and .331 respectively. The band parameters $\eta=1$, $M/m=25$ and $\alpha=5$ give a narrow oscillator band. Energy transfers are plotted about the origin $n\omega_o$. The unbroadened line at $n\omega_o$ which we do not plot has a weight relative to the plotted $\hat{S}_-(Q,\omega)$ given by the Debye-Waller factor. $\tilde{S}_-(Q,\omega)$ is defined by equation (6.5) and has the unbroadened line subtracted out. The relevant Debye-Waller factor is discussed in the text following (6.5).

Figure 4

$\hat{S}_-(Q,\omega)$ against energy transfer (ω). The temperature is $T^*=2$ as in the second plot of figure 3, but now $Q=4$. The band parameters and details of the plot are as in figure 3. Note the much greater width at higher Q (the energy scale is increased) but also the clear remnants of the structure of the lattice band. The broken line is the Gaussian approximation referred to in the text.

Figure 5

$\tilde{S}_-(Q,\omega)$ against energy transfer (ω). The details of the band parameters and the plot are as in figure 3. Temperature remains at $T^*=2$ but $Q=5$. The width is now much greater and features from the band are almost blurred out. The broken line is the Gaussian approximation.

Figure 6

$\tilde{S}_-(Q,\omega)$ against energy transfer (ω). The details of the band and the plot are as in figure 3. $T^*=2$ and Q is further increased to 6. The Q value is now sufficient to remove the structure in $\tilde{S}_-(Q,\omega)$ (except around the peak) by favouring multi-quanta processes. The Gaussian approximation, indicated by the broken line, is a very good fit to the actual $S_-(Q,\omega)$, the shape on the upper frequency side being essentially exact. There is a slight mismatch in the peak positions, in other words, in the recoil estimates. A slight asymmetry is also evident.

Figure 7

$\tilde{S}_-(Q,\omega)$ against energy transfer (ω). The case of a wide oscillator band (parameters $\eta=1$, $\alpha=.9$, $M/m=5$) is plotted for $Q=.1$ and $T^*=.1$. At such low Q and T^*, $\tilde{S}(Q,\omega)$ is essentially $Q^2Z(\omega)C(\omega)/\omega$ for each band that is being plotted. Up-scattering is weak and thus only positive energy transfers are shown. The Debye-Waller factor is .766 indicating that only ~25% of the total intensity is in the shifted and broadened components shown and ~75% is in the unbroadened elastic line not shown. The $\tilde{S}(Q,\omega)$ is now the structure factor resulting from both bands, the tilde again indicating subtraction of the delta function component.

Figure 8

$\tilde{S}_-(Q,\omega)$ against energy transfer (ω). The band parameters are as in figure 7. At $Q=1$, $T^*=1$ of the figure, $\tilde{S}(Q,\omega)$ shows appreciable multi-quanta processes. The peaks characteristic of the lattice and oscillator bands around .75 and 1.65 are shown to be repeated at the (roughly) harmonic positions. The Debye-Waller factor is now .0532 indicating that ~95% of the intensity in $S(Q,\omega)$ resides in the plotted structure factor. The width of the lower order lines in $S(Q,\omega)$ is around 1/4 of the characteristic energy of the lattice,

that is, around 6 meV for typical systems. A definite smooth background underlies the sharp peaks.

Figure 9

$\tilde{S}(Q,\omega)$ against energy transfer (ω). Momentum transfer Q remains =1 as in figure (8) but $T^*=2$. Doubling the temperature reduces the peak intensities (note the different scale for $\tilde{S}(Q,\omega)$ from figure (8)) and slightly increases the background. Peaks beyond -2 and +4 have increased greatly.

Figure 10

$\tilde{S}(Q,\omega)$ against energy transfer (ω). Temperature $T^*=2$ remains at the value of figure (9). Wavevector Q is increased to 1.5 with the effect that the background becomes much broader (the energy transfer scale is increased). There is now a clear shift. The background is much the same level as in figure (9) but the peaks have decreased in intensity. The broken line indicates the Gaussian approximation of the text and has a width of 2.729 and a shift of 1.838.

Figure 11

$\tilde{S}(Q,\omega)$ against energy transfer (ω). Temperature remains at $T^*=2$ (as in figures (9) and (10)) and wavevector is further increased to Q=2. The background is now closer to the broken line of the Gaussian approximation (width=3.638, shift=3.267) and decreasing intensity of the peaks makes them less well-resolved from the background. Further increases in Q rapidly accelerate this transition of $\tilde{S}(Q,\omega)$ to the Gaussian form via the reduction in individual peak intensities.

Figure 12

The limits of integration of μ and λ. The plane of constant ω is limited by its intersection with a unit cube in S-space, the actual resultant shape depending upon the value of $\zeta(\omega)$, labelling each figure, which is the perpendicular distance from the origin to the plane. The variables μ and λ define an orthogonal coordinate system within the bounded planes as indicated for example in the figure for $\zeta=1.2$. The value of η chosen for the figures is $\eta=.4$. The limits of integration on μ are given against each figure as are

the ranges of ξ that each figure represents. The appropriate form of the function $H(\mu)$ to be taken can easily be seen by inspection of each figure and the attached indication of the range of values of μ.

1

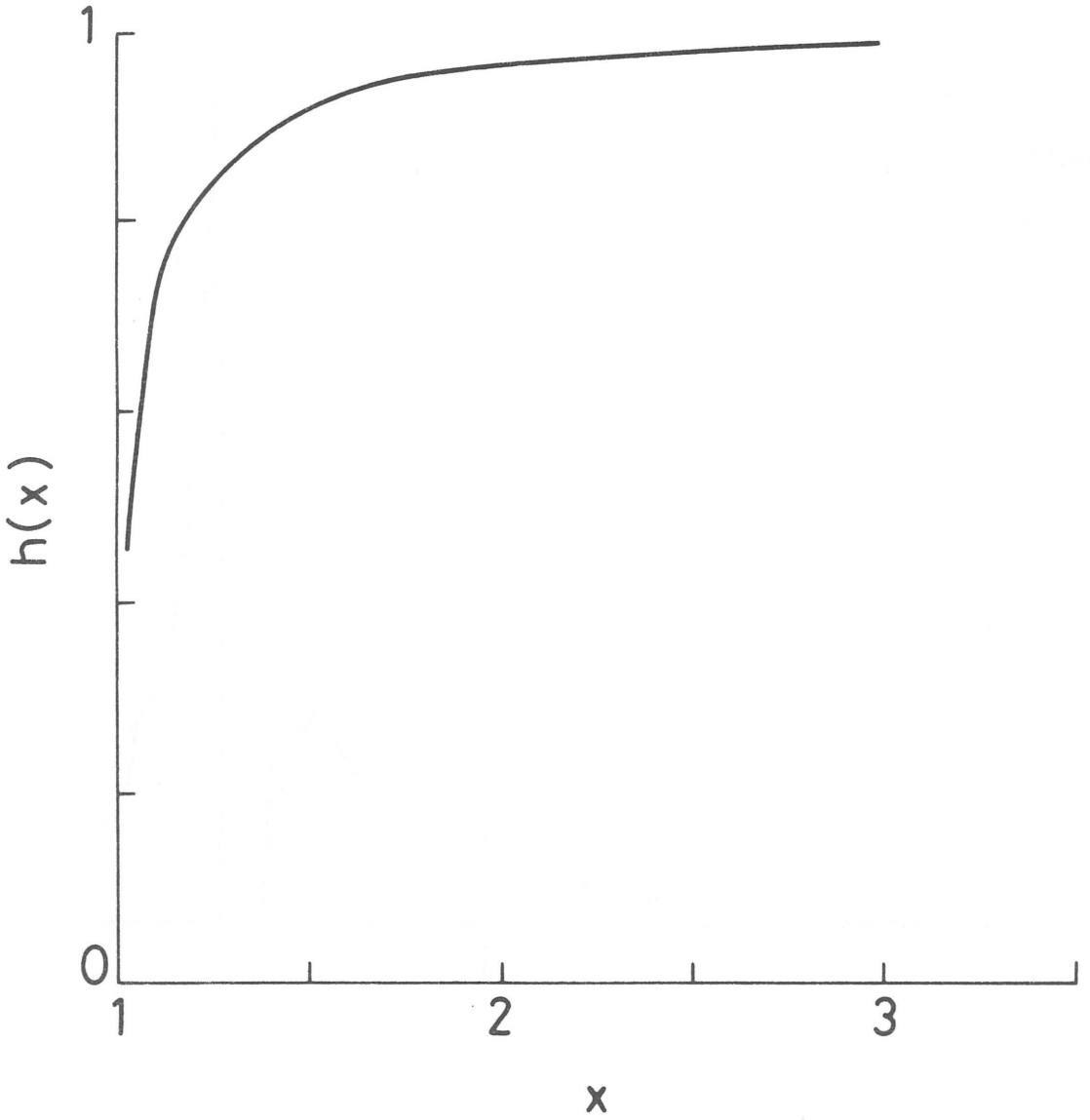

2

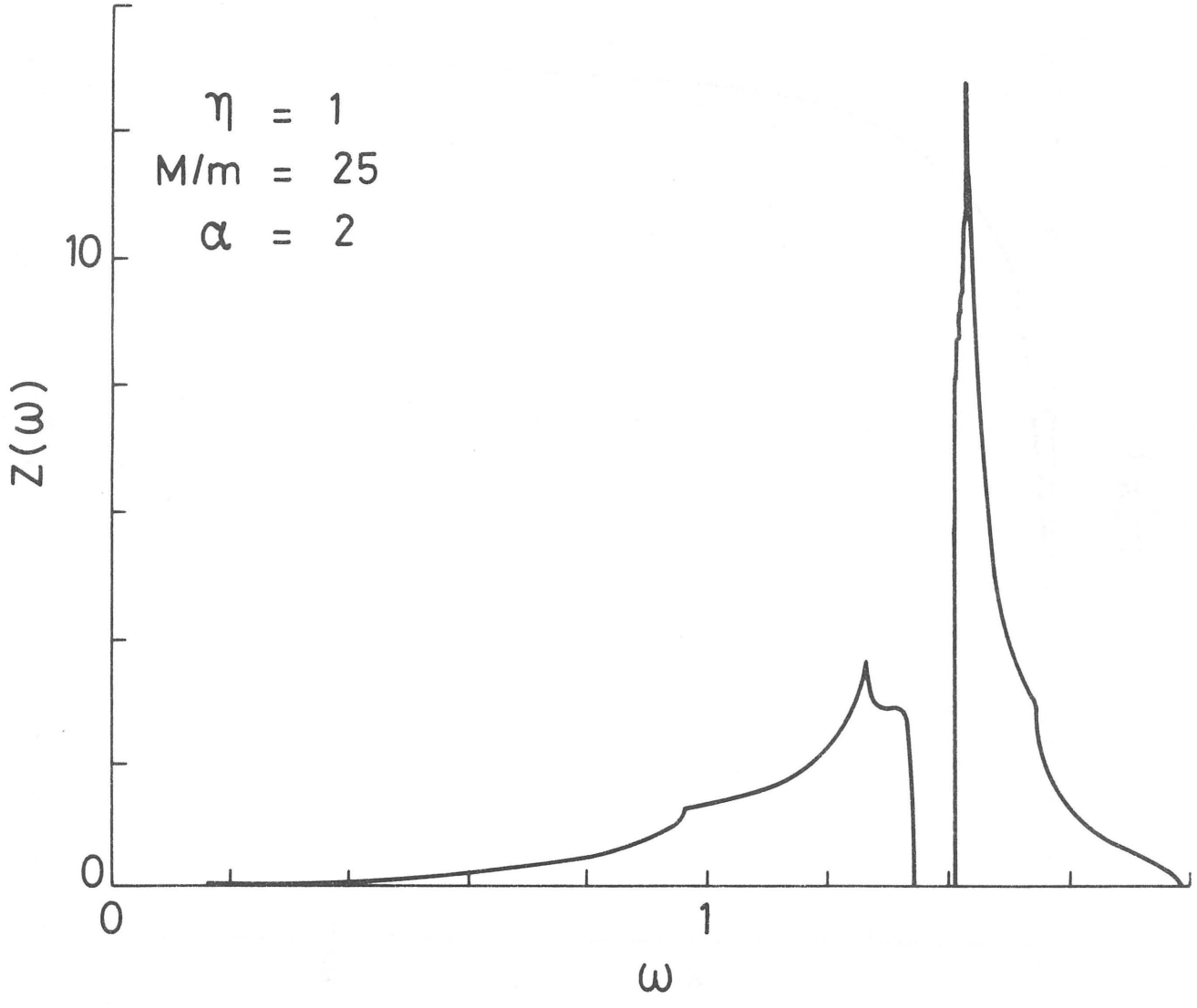

3

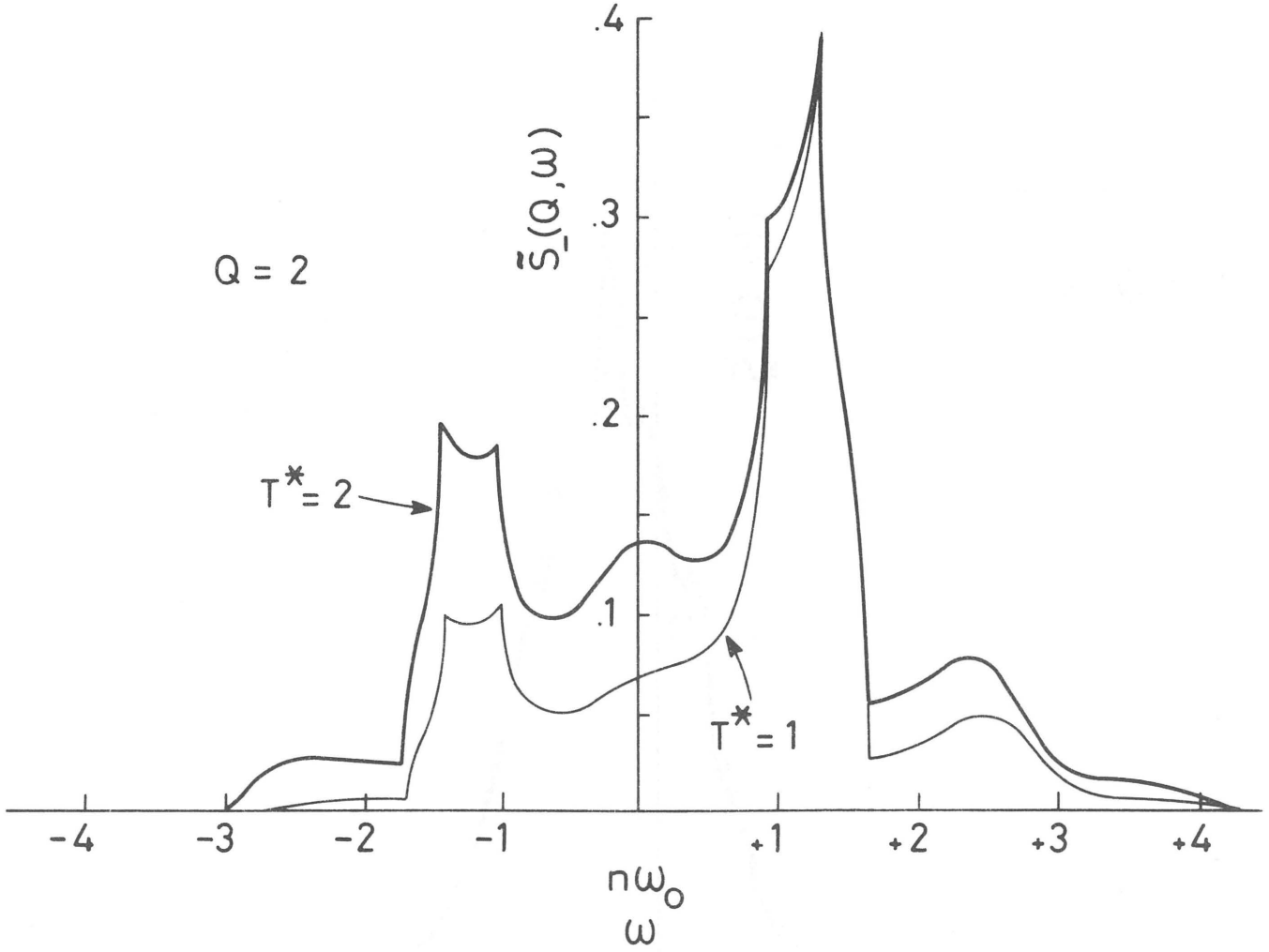

4

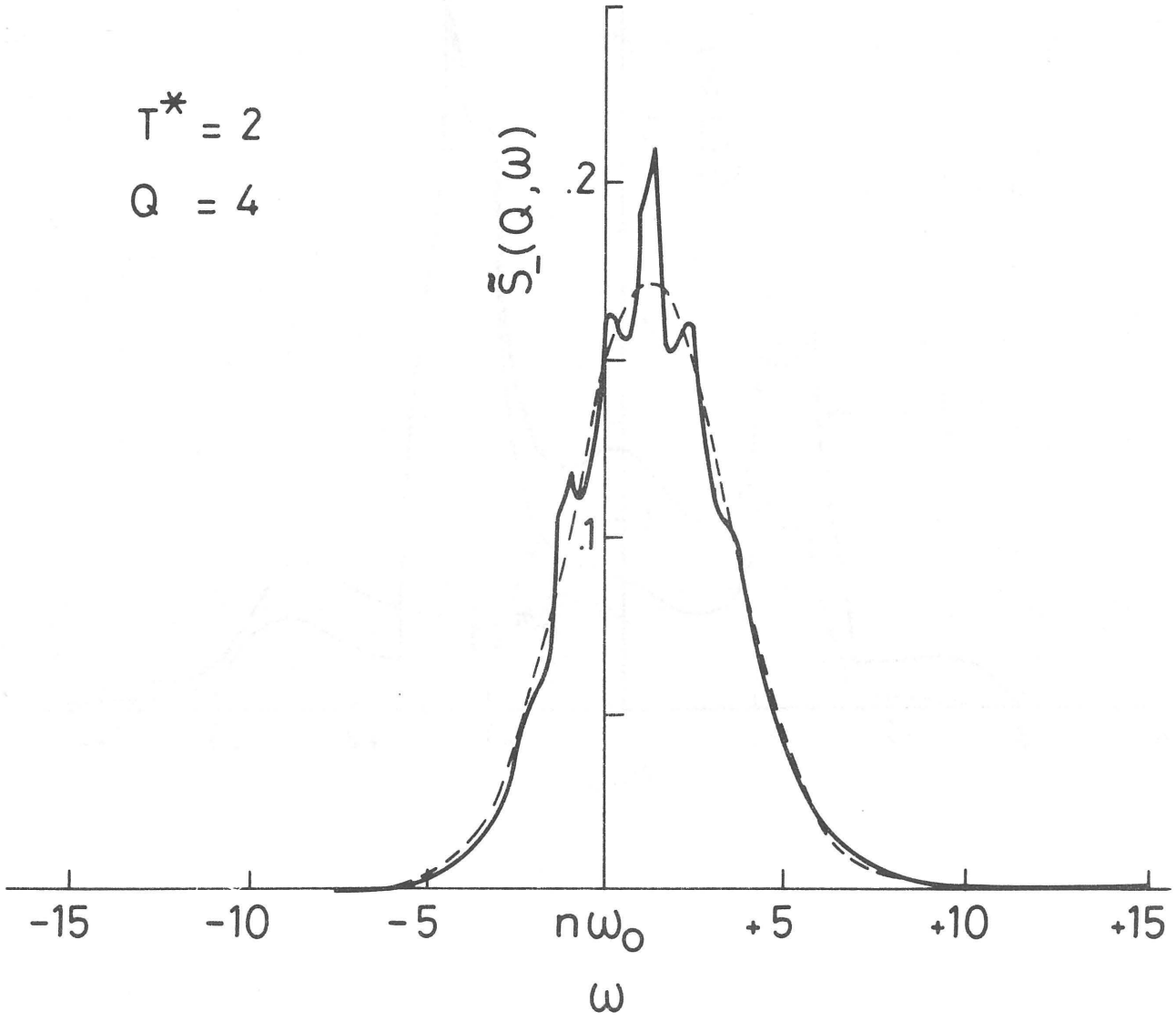

5

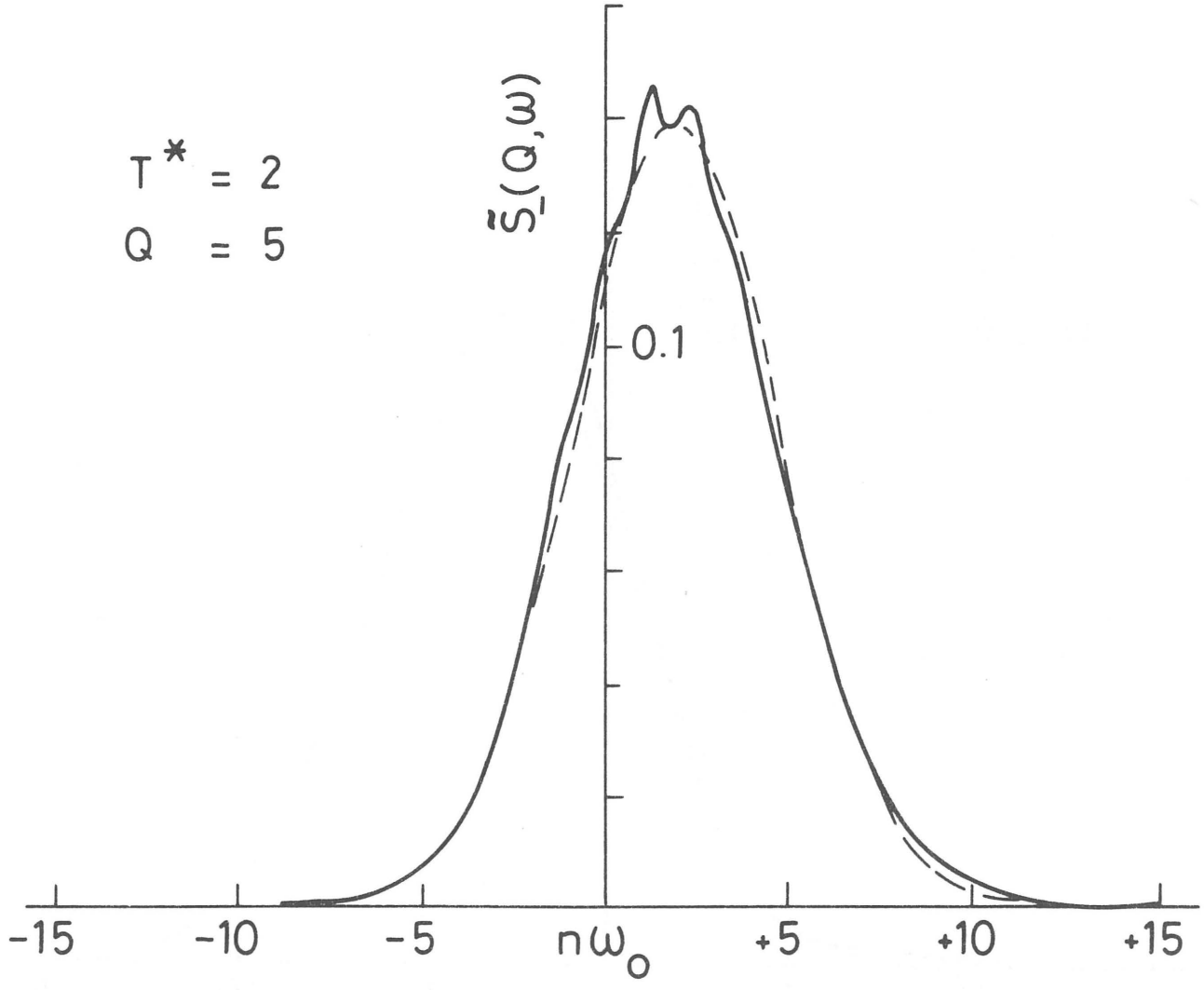

6

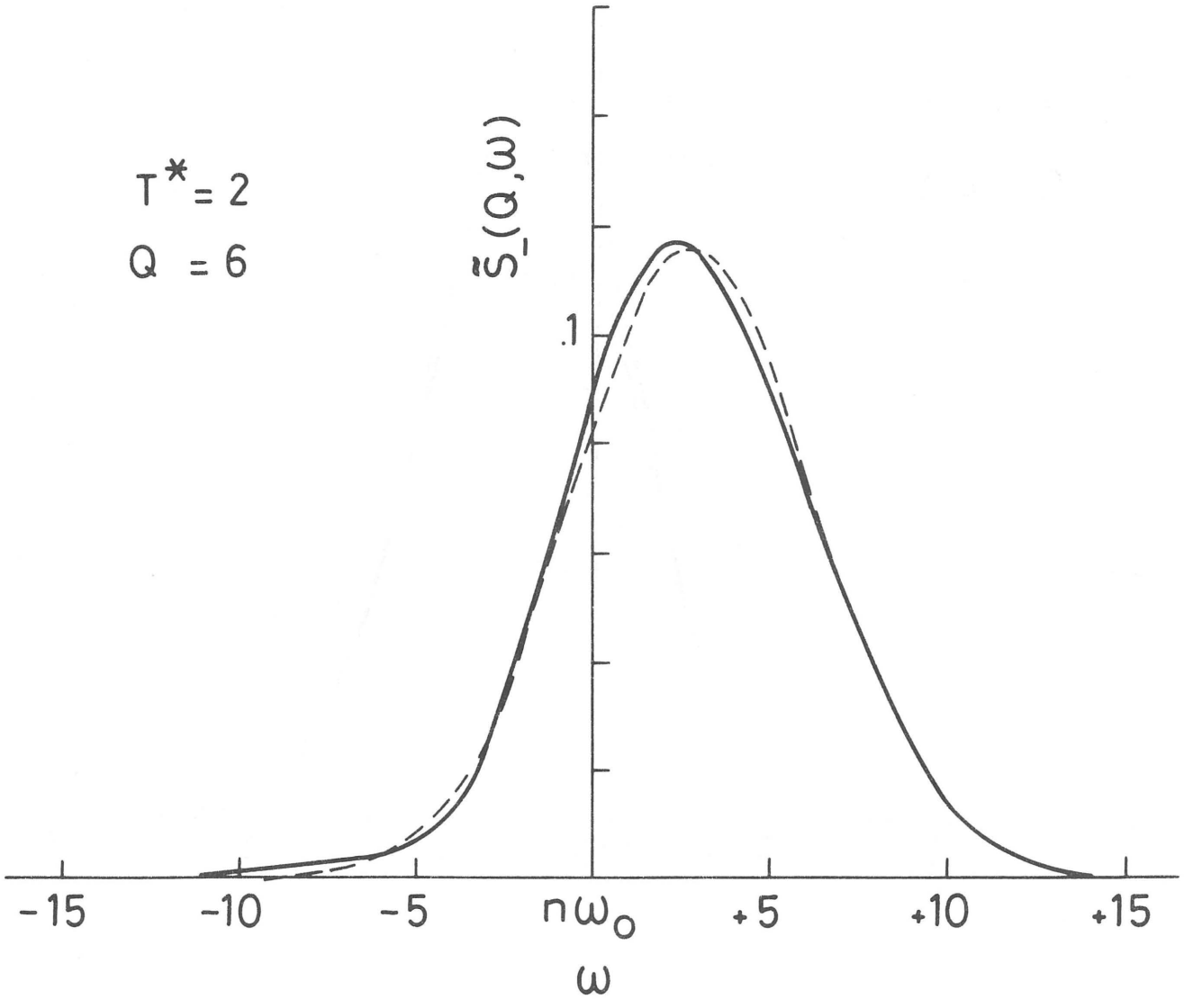

7

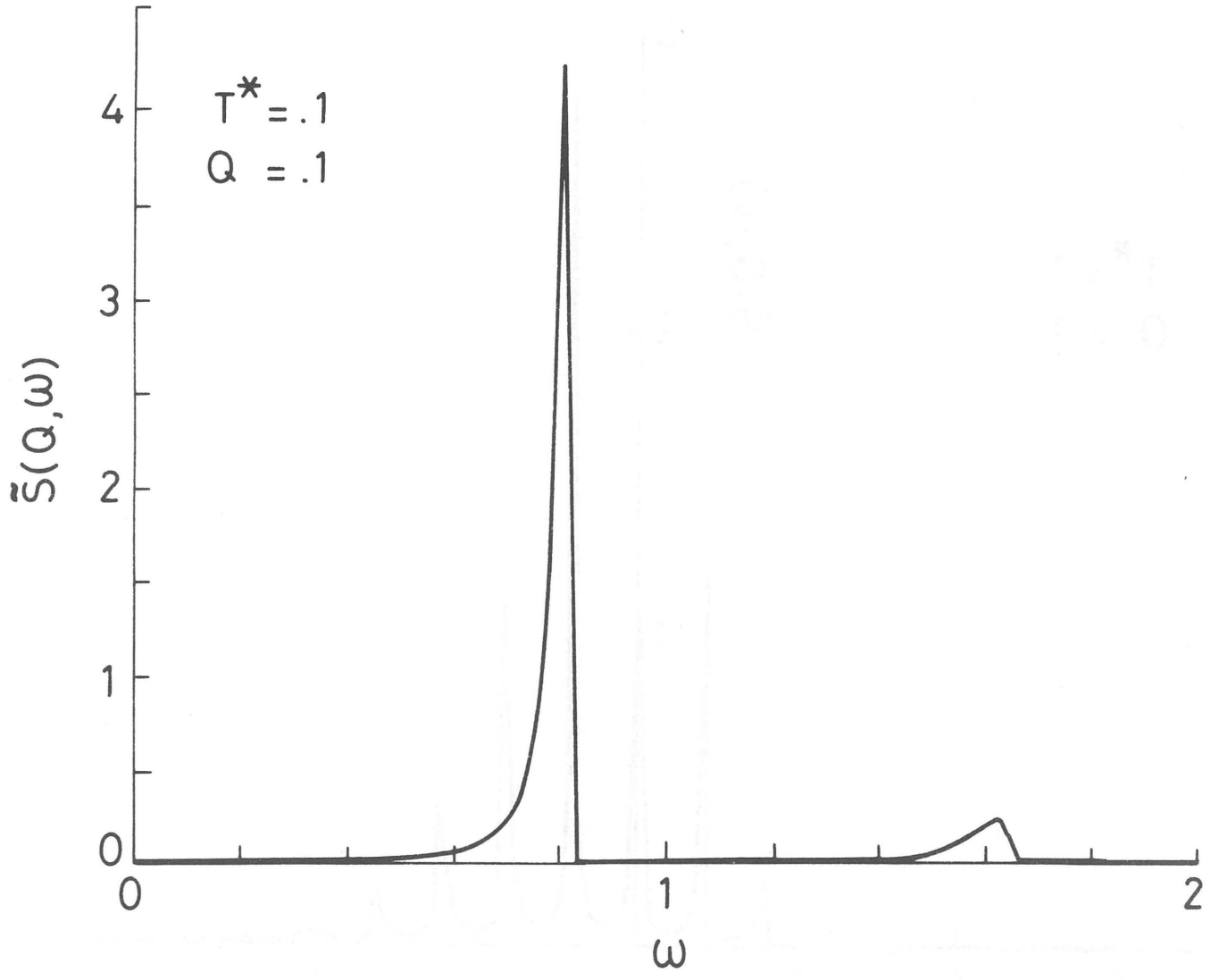

8

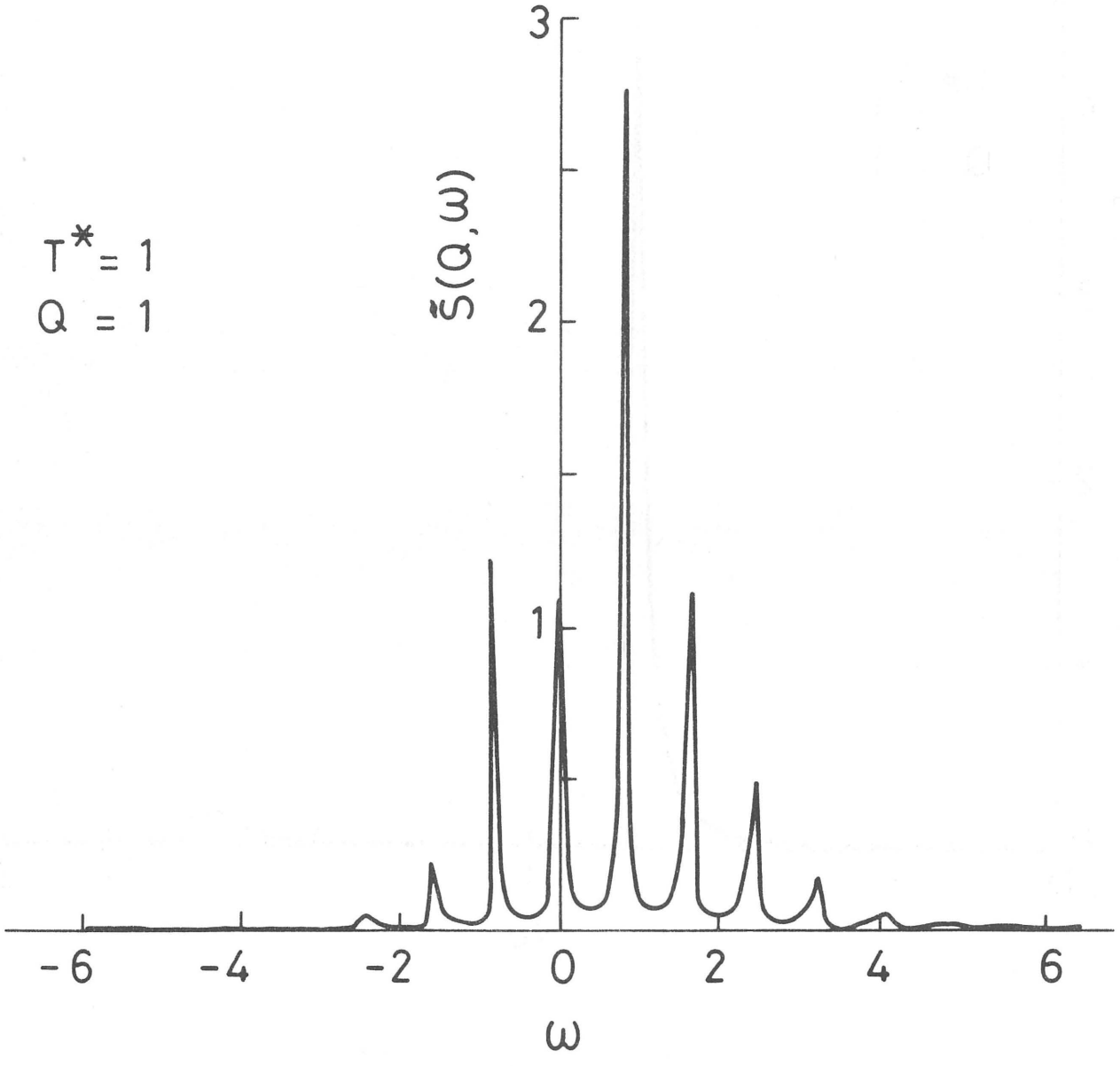

9

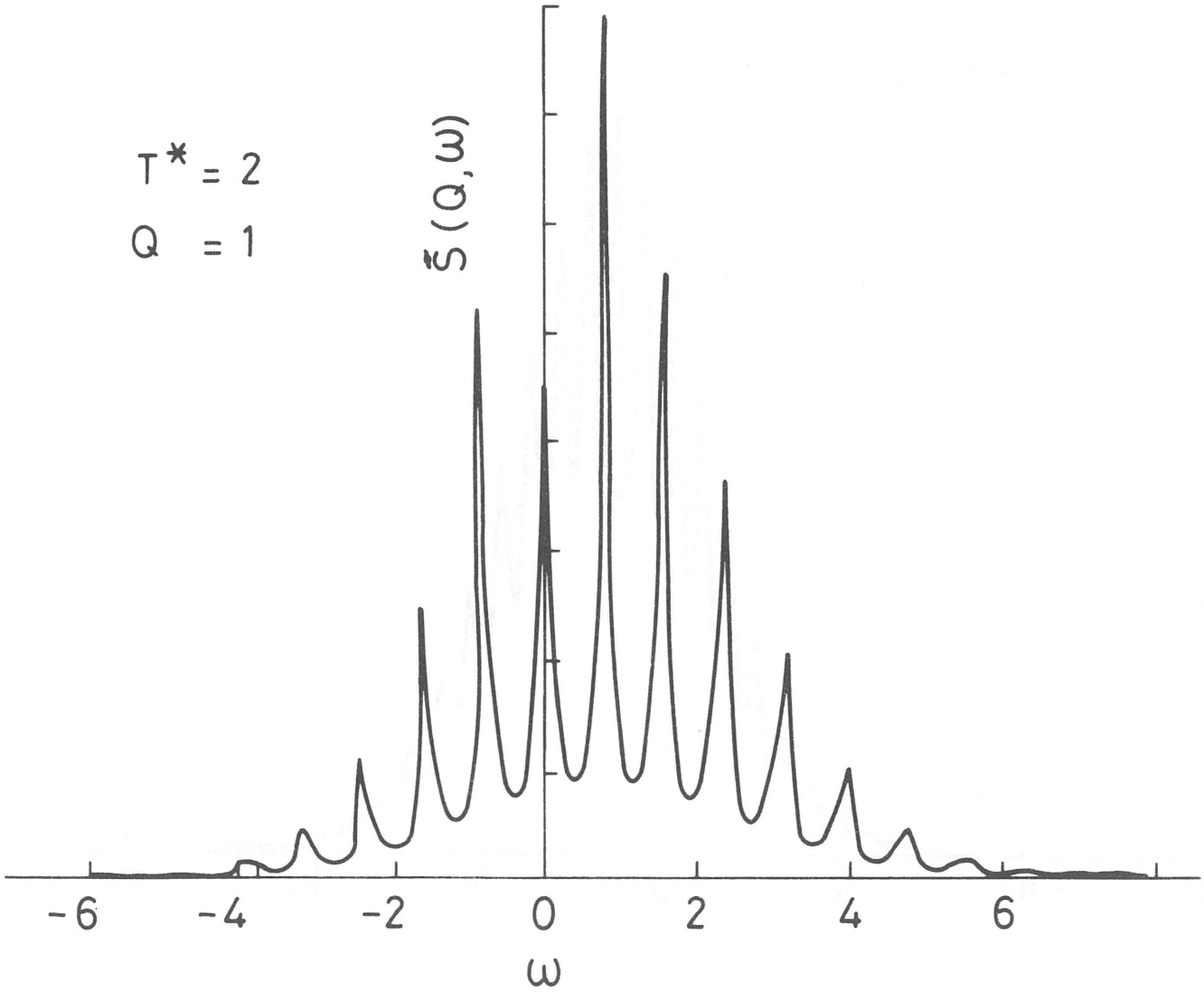

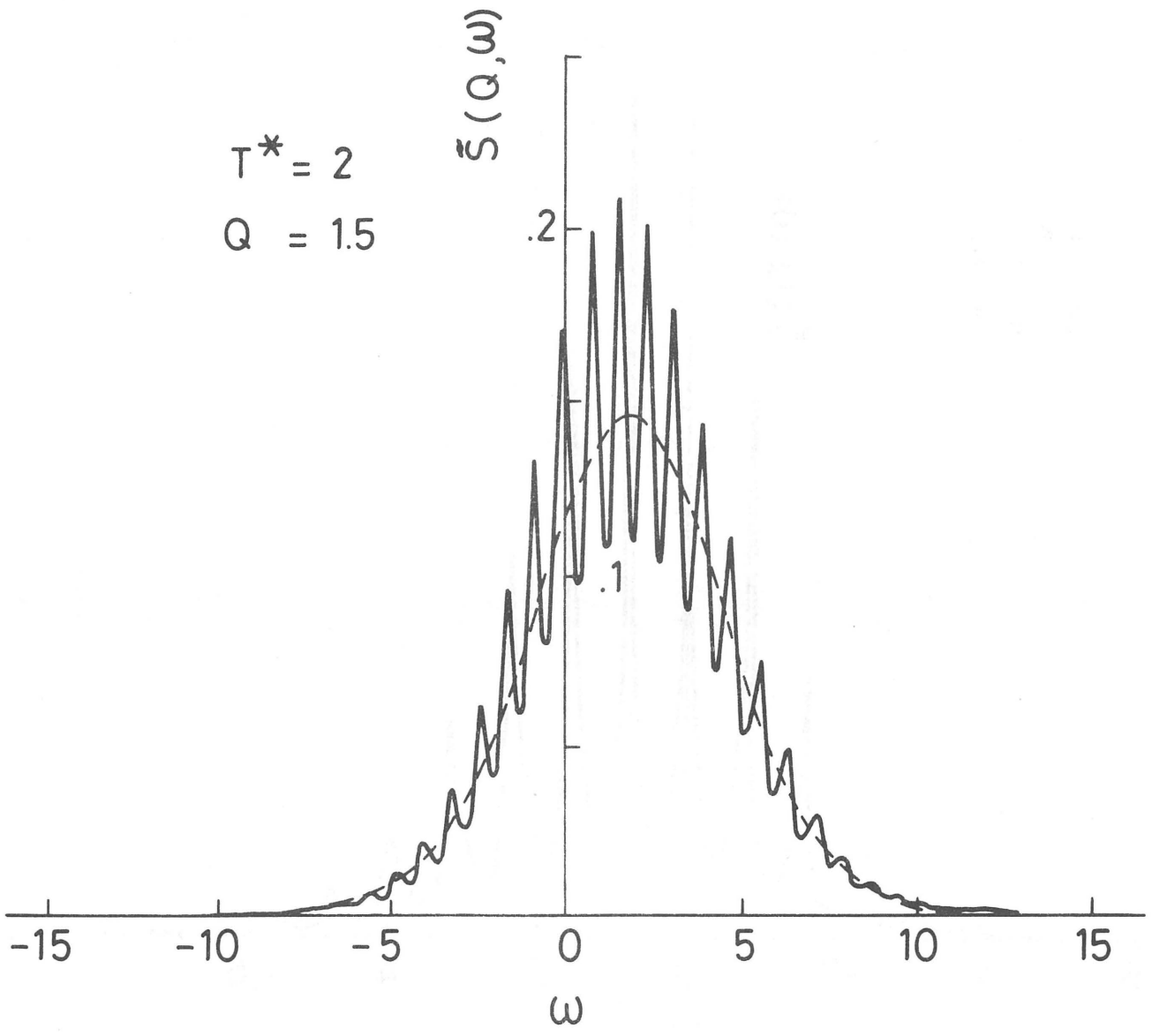
T* = 2
Q = 1.5
S(Q,ω)
.2
.1
-15
-10
-5
0
5
10
15
ω

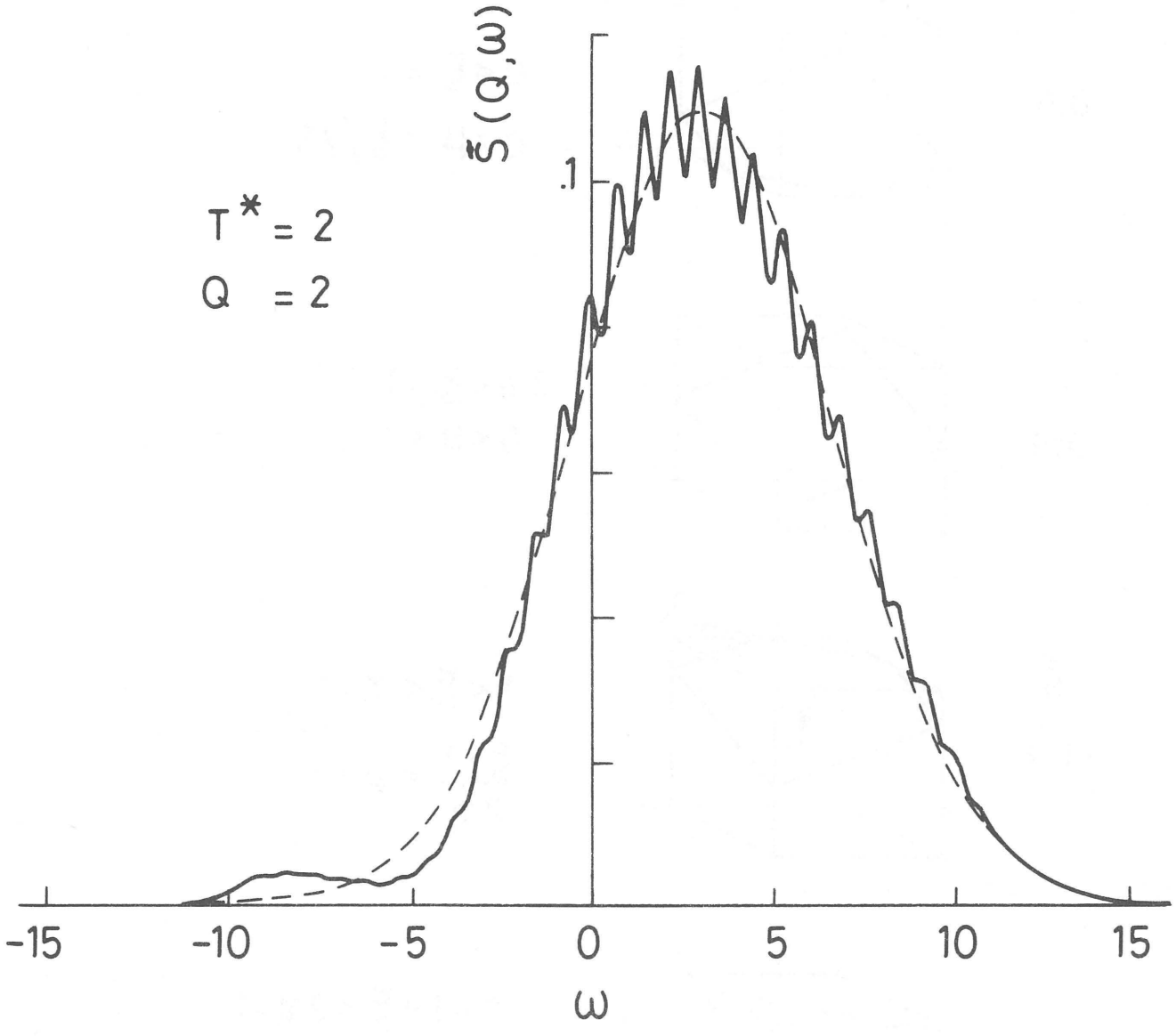
S(Q,ω)
.1
T* = 2
Q = 2
-15
-10
-5
0
5
10
15
ω

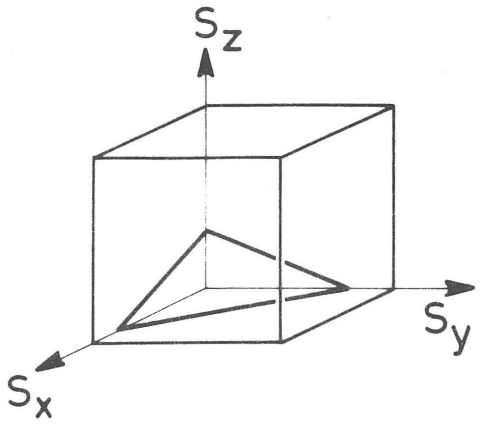

ξ

0.3

$0 < \xi < \eta$

$0 < \mu < \xi / 2\eta$

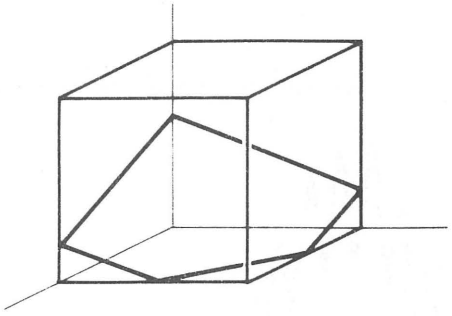

0.6

$0 < \xi < \eta$

$0 < \mu < \xi / 2\eta$

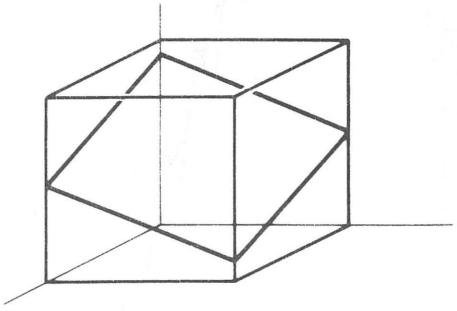

0.9

$2\eta < \xi < 1$

$0 < \mu < 1$

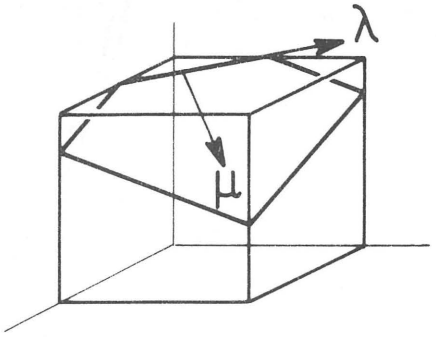

ξ

1.2

$1 < \xi < \eta + 1$

$\frac{\xi - 1}{2\eta} < \mu < 1$

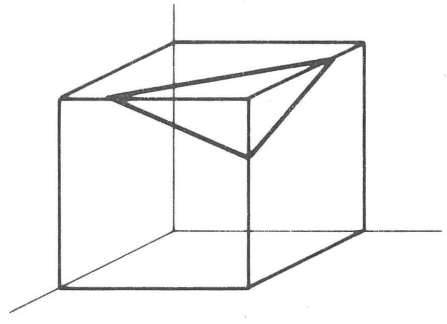

1.5

$\eta + 1 < \xi < 2\eta + 1$

$\frac{\xi - 1}{2\eta} < \mu < 1$